Journal of Hydrology 570 (2019) 185–200

Contents lists available at ScienceDirect

Journal of Hydrology

journal homepage: www.elsevier.com/locate/jhydrol

Quantifying the wetland water balance: A new isotope-based approach that includes precipitation and infiltration

Edward K.P. Bam*, Andrew M. Ireson

School of Environment and Sustainability and Global Institute for Water Security, University of Saskatchewan, Saskatoon, SK, Canada

ARTICLE INFO

This manuscript was handled by Marco Borga, Editor-in-Chief, with the assistance of Huade Guan, Associate Editor

ABSTRACT

Stable isotopes have been used to quantify lake and wetland pond water loss to evaporation by applying the modified Craig and Gordon (1965) model. This model and its derivatives employ simplifying assumptions that ignore the additions of precipitation and infiltration outputs and assume evaporation is the only loss term over the prediction period. Here we develop a coupled water and isotope mass-balance model to account for precipitation additions. Our model uses physical and isotopic observations to quantify pond evaporation and infiltration losses over the ice-free period. We tested and applied the model to four wetland ponds at the St Denis National Wildlife Research Area, Saskatchewan Canada, where we have long-term datasets. Modeled infiltration rates from the ponds ranged between 0.99 and 9.2 mm/d and open water evaporation rates ranged between 0.88 and 2.8 mm/d. Both were consistent with independent estimates. Infiltration amounts were highest in the ephemeral ponds (that dry out within days or weeks of the spring melt period). In these ponds, infiltration exceeded evaporation. In permanent ponds, that is ponds that do not dry out; evaporation exceeded infiltration. Evaporation amounts were most substantial for permanent ponds that were not sheltered by topography or riparian vegetation. Overall, our coupled water and isotope mass-balance model combined with physical and isotope observations was able to quantify the spatially and temporally variable evaporation and infiltration fluxes within and between ponds.

1. Introduction

Wetlands provide essential ecosystem services, including flood mitigation, groundwater recharge, sediment and pollutant trapping, and fish and wildlife habitat. Wetland ponds (defined as open water areas within wetlands) serve as important sources of food and breeding grounds for migratory birds and other living organisms (Bortolotti et al., 2013). In the Great Plains of North America, there are millions of wetland ponds in the so-called Prairie pothole region (Hayashi et al., 2016; Hayashi and Van Der Kamp, 2000; Steinman et al., 2010). The eco-hydrological functionalities of these wetlands in this semi-arid climate depends on the seasonal water cycle dynamics (Jolly et al., 2008; Labaugh et al., 1997, 1996; LaBaugh et al., 2016; van der Kamp et al., 2008; van der Kamp and Hayashi, 2009; Winter, 2000). Accurate estimation of water budget components and the accompanying physical and chemical changes in a wetland pond, groundwater, and riparian zone are essential for calibration and validation of hydrological and biogeochemical models.

Wetlands form in topographic depressions, and within the wetland there is often a pond. There are five types of wetland ponds found in the North American Great Plains. Type 1 and 2 ponds (often called temporary or ephemeral) are formed in shallow depressions as free surface water after snowmelt or storm events in early spring and summer. These may last only a few days or weeks but dry up in the summer. Type 3 ponds (also known as seasonal ponds) are characterized by shallow marsh vegetation, which generally occurs in the deepest part of the pond. These ponds dry up by midsummer. Type 4 ponds (also known as semi-permanent ponds) maintain surface water throughout the growing season, i.e., from May to September but lack persistence most of the year. They are dominated by marsh vegetation at the central zone of the wetland, as well as coarse emergent plants or submerged aquatic species, including cattails, bulrushes, and pond weeds. Finally, Type 5 ponds (also referred to as permanent ponds) are ponds that always hold a large volume of open water for most years in the central zone of the pond. They are generally devoid of vegetation, but submerged plants may be present in the deepest zone, while emergent plants (such as cattails, red swampfire, and spiral ditch grass) are often found along the edges (Stewart and Kantrud, 1971).

The water balance of wetland ponds is controlled by meteorological forcing and subject to substantial seasonal and inter-annual variability

* Corresponding author at: Global Institute for Water Security, University of Saskatchewan, 11 Innovation Boulevard, S7N 3H5, SK, Saskatoon, Canada.
E-mail address: e.bam@usask.ca (E.K.P. Bam).

https://doi.org/10.1016/j.jhydrol.2018.12.032
Received 1 February 2018; Received in revised form 23 December 2018; Accepted 24 December 2018
Available online 29 December 2018

caused by spatially and temporally variable surface and subsurface processes (Hayashi et al., 2016; Jolly et al., 2008; van der Kamp and Hayashi, 2009). In seasonal drought-prone climates like the Prairies, pond water balances and water residence times are controlled by climate variables and pond area, volume, and shape (Benson and Paillet, 1989; Hayashi et al., 2016; Steinman et al., 2010). Ponds can be fed by direct precipitation, snowmelt- and rainfall-runoff, channelized inflows, and groundwater discharge. Ponds lose water by evaporation, infiltration, and spillage. The spillage occurs when storage exceeds a local threshold usually from either overland flow or channelized outflow (Spence and Woo, 2003; Spence, 2010). Pond water infiltration may be transpired by the riparian zone plants, lost as soil evaporation, and serve as recharge water to the underlying groundwater system. The direction of surface water-groundwater interactions varies spatially as a function of landscape position and elevation relative to the groundwater heads, and temporally as a function of seasonal and inter-annual meteorological forcing (Brannen et al., 2015; Leibowitz et al., 2016; Leibowitz and Vining, 2003).

The water balance is the dominant, but not exclusive, control on the water chemistry of a wetland pond. Hence, seasonal and inter-annual changes in pond water chemistry are often explained by dilution by precipitation (rainfall over the pond) or salt enrichment by evaporation (Goldhaber et al., 2014; Heagle et al., 2007; Labaugh et al., 1997; Pennock et al., 2014). Water balance controls on the chemistry of a wetland pond include solute inputs from land surface runoff into the pond, plant transpiration, and sometimes groundwater discharge, and solute outputs to groundwater recharge and/or spill (Dogramaci et al., 2015; Goldhaber et al., 2016; Leibowitz et al., 2016; Leibowitz and Vining, 2003; Nachshon et al., 2014). Ponds that tend to lose water to the groundwater system (i.e. groundwater recharge ponds) have lower salinities than ponds that gain water from the groundwater system (i.e. groundwater discharge ponds) (Labaugh et al., 1998; Nachshon et al., 2014; Salama et al., 1993; Sloan, 1972). The long-term fluctuations in the chemistry of wetland ponds are caused by multi-year, wet-dry variations associated with meteorological forcing in the region (Cressey et al., 2016; Goldhaber et al., 2016, 2014; LaBaugh et al., 2016). Nachshon et al. (2014) showed that extreme wet conditions could cause groundwater discharge and surface runoff of salts from an upland area into freshwater ponds resulting in freshwater ponds becoming salinized. Inadequate knowledge of the climate history and chemistry of a particular pond, therefore, could lead to a misdiagnosis of the pond's hydrological function by short-term observations of pond water chemistry. In addition to these water balance controls, geochemical and biochemical interactions within a wetland pond and underlying wetland soils may add or remove solutes from the wetland pond water (Heagle et al., 2007; LaBaugh et al., 2016; Pennock et al., 2014). The implications of these high degrees of spatial and temporal variability, combined with complex biogeochemical processes that occur within wetland ponds, make it difficult to use chemical ions/solutes as useful tracers for estimating hydrological fluxes in such terrain.

On the other hand, stable isotopes, which are part of the water molecule, are also controlled by the water balance. However, unlike solutes, stable isotopes are unaffected by geochemical and biogeochemical processes in most non-geothermal environments and therefore serve as powerful tracers for hydrological studies (Geyh et al., 2000). Studies involving the qualitative and quantitative analysis of stable isotopes of surface water bodies have been reported in the Prairie Pothole region of North America (Fritz et al., 1987; Gammons et al., 2006; Gibson et al., 2005; Pham et al., 2009; Steinman et al., 2010; Wassenaar et al., 2011). These studies show that seasonal stable isotope variability within the surface water body is significant and contains useful information about the local hydrological processes. But to date, few studies (Gat and Levy, 1978; Pham et al., 2009; Steinman et al., 2010) have used stable isotopes to describe the variability in hydrological function the of different wetland ponds in the Prairies and similar, seasonally cold semi-arid regions.

Globally, quantitative models (Gibson et al., 1993, 1996, 2016; Gibson et al., 2016; Gilath and Gonfiantini, 1983, 1986; Jones et al., 2005; Jones and Imbers, 2010; Skrzypek et al., 2015; Steinman et al., 2010) based on the isotope-evaporation equation of Craig and Gordon (1965) and the large lake water-budget equation (e.g., Gonfiantini (1986) have been used to describe surface water response to meteorological forcing and to estimate the evaporation to water input ratios in data scarce regions or interpret paleoclimate conditions. These models consider the initial and final isotope composition, climate data, atmospheric water vapour isotope compositions, and assume that no new additional water source is added during the study period (Gibson et al., 1993; Skrzypek et al., 2015). The outputs are the fraction of water lost to evaporation or evaporation-inflow ratios in the case of flowing streams or rivers. Thus, in such model formulations, the effect of isotope inputs from isotopically distinct water (e.g., rainfall or surface inflow) and the volume additions to the system at the time of computing these fractions or evaporation-inflow ratios are negligible. These assumptions have been justified on the basis that the lake and river volumes were too large to be affected by such additions (Skrzypek et al., 2015). In the existing models, leakage under the water body (i.e., water lost by infiltration) is negligible, and surface area-volume ratio remains constant even as the water levels decline with time. Overall, these assumptions are problematic for areas where rainfall over small lakes and ponds are significant, where ponds leak through infiltration, and when water levels decline or increase. These changes can significantly alter the isotope composition of the surface water body and could significantly impact the flux estimates produced from the existing models.

In some previous studies (e.g., Gibson, 2002a,b; Gibson et al., 2016; Gilath and Gonfiantini, 1983; Gonfiantini, 1986), the idea to include volume and isotopic changes, basin area and shape, and infiltration components into the model has been discussed. Later studies involving individual modelling experiments (e.g., Gibson et al., 2016; Gibson, 2002a,b; Jones et al., 2005; Steinman et al., 2010) have incorporated some or all three factors into the model formulation. These new formulations, however, were done on limited scales to suit local needs and, therefore, difficult to generalize and apply elsewhere. For example, to reduce the uncertainty in evaporation-inflow ratios, Gibson (2002a,b) estimated and incorporated lake shape and size parameters into the water balance equations when considering the different lakes of northern Canada. Jones et al., (2005) addressed the effect of basin shape and surface area changes in the model to recalibrate isotope records from a lake in Nar Golu in Turkey. Steinman et al., (2010) considered the effect of infiltration under cone-like lakes and also implemented the geometric changes associated with the surface area to volume changes in a paleoclimate study in the upper Columbia River basin of the United States. Rozanski and Chmura (2008) in a laboratory study showed that a key parameter controlling isotopic enrichment is leaking containers is the remaining fraction of water in the container. Thus these findings suggest collectively that neglecting the impact of infiltration, pond shape, size, and the surface area to volume ratio of small water bodies in estimating evaporation fluxes from isotope-water-mass balance models will result in significant errors of the individual water balance components.

In this work, we take the critical next step to develop a new physically-based isotope-water-mass balance model that takes into consideration inputs from precipitation and losses to infiltration with accompanying bathymetry changes in a generalizable model. Our goal is to interpret the differences in stable isotope composition of various types of wetland ponds and hence to describe their differing hydrologic regimes. We leverage two decades of hydrometric, climate, and isotope data collected from a variety of Saskatchewan wetland ponds to understand, and model the isotopic changes and estimate water mass balance components of the Prairie wetlands. We perform this work at the well-studied St Denis National Wildlife Area (Bortolotti et al., 2013; Hayashi et al., 2016; Nachshon et al., 2014; Pennock et al., 2014; van der Kamp and Hayashi, 2009), near Saskatoon. Our objectives are to: i)

Fig. 1a. Location of the Prairie Pothole Region in the midcontinent of North America (adapted and modified from van der Kamp and Hayashi (2009)).

explore the stable isotope composition records of wetland ponds to characterize their hydrologic function; ii) develop a new coupled physically based isotope and water mass balance model that takes into account rainfall additions (which result in volume and isotope composition changes) and different pond geometries for the ice-free summer season and accounts for infiltration losses; iii) test the model sensitivity to changing pond geometries and climate parameters; and iv) compare the model results with independent estimates of evaporation, infiltration, and storage from existing methods and isotope-water mass balance models where feasible.

2. Study site and field methods

2.1. The study site

Field data was collected between May and October starting in 1994 at the 385-ha St. Denis National Wildlife Area, SDNWA, (52.8 N, 106.8 W) in the Canadian Prairies (Fig. 1a). The area and location of wetlands at the SDNWA is shown in Fig. 1b with the wetlands studied identified in numbers. The site is 40 km east of Saskatoon, Saskatchewan, Canada. The SDNWA was established in 1968 as a long-term study site for the environmental and ecological monitoring of the prairie wetland complex (Hogan and Conly, 2002). There are close to one-hundred ponds of varying size and hydrological seasonality at the SDNWA (Woo and Rowsell, 1993; van der Kamp and Hayashi, 2009). The climate is semi-arid with significant inter-annual variability in precipitation and temperature during the summer (April–September) and winter (October–March) months. The mean annual non-adjusted (for wind-caused under-reported winter snowfall) precipitation at Saskatoon is 360 mm, with about 280 mm occurring as rainfall in April–October (Nachshon et al., 2014; Parsons et al., 2004). The monthly mean temperature varies between −14.7 °C in the period December to February and 18.7 °C in the period between July and August (Wittrock and Beaulieu, 2015). Just like other prairie sites, the annual lake evaporation exceeds the total annual precipitation (Parsons et al., 2004).

The arithmetic mean estimate for a twenty-four year monthly integrated record of isotopes in precipitation for Saskatoon is −17.0‰ and −131.0‰ for $\delta^{18}O$ and $\delta^{2}H$, respectively. The amount-weighted mean values of $\delta^{18}O$ and $\delta^{2}H$ for the period June 1990–November 2014 are −14.4‰ and −112.5‰, respectively. The summary of the values of monthly amount precipitation, temperature, $\delta^{18}O$, $\delta^{2}H$ and the local Saskatoon meteoric water line for the period 1990–2014 is given in Fig. 2. The monthly integrated isotopes in precipitation data is available in Bam et al. (2018).

The study was conducted at pond 50, 109, 117 and 120. The wetlands were selected based on previous wetland pond classification of Stewart and Kantrud (1971): Ephemeral pond (117); Semi-permanent pond (120); and Permanent pond (109 and 50). Ponds 109, 117 and 120 can be described as “recharge ponds” since they have hydraulic head values that are elevated above the potentiometric surface of the underlying confined aquifer system (Bam, 2018). Pond 50 has a hydraulic head that is more-or-less at the same head stage with the underlying regional intertill aquifer and is therefore neither a recharge pond nor a discharge pond (Bam, 2018). A hydro-meteorological tower near pond 109 on the site collects half-hourly measurements of air temperature, relative humidity, and precipitation at 2 m and 10 m heights for the 2014 season.

2.2. Hydrological measurements

The water level in the pond was measured manually, and in later years using logged pressure transducers, at georeferenced poles installed within the wetlands (Conly et al., 2004). The measured water levels were converted to depth of water (in meters) at the deepest location in the wetland. The area, A (m^2), and volume, V (m^3), of surface water stored in the wetland was estimated using the equations described in Hayashi and Van Der Kamp, (2000) and Hayashi et al., (2016) as a function of water depth, k (m):

$$A = sk^{2/\beta} \quad (1)$$

$$V = \frac{sk^{(1+2/\beta)}}{1 + 2/\beta} \quad (2)$$

where s (m^2) is a scale parameter (equal to the pond surface area when the depth is 1 m), and β is parameter the defines the shape of the idealized pond cross section, where $\beta = 1$ is an inverted cone, $\beta = 2$ is a parabola, and larger values represent a bathtub-shaped basin with a flat bottom and steep sides (Hayashi and van der Kamp 2000). The constants s and β were determined using bathymetry survey data of ponds 50, 109, 117, and 120 (see Hayashi and Van der Kamp, 2000; Heagle et al., 2013) and updated survey of 2009 (van der Kamp pers. Commun.). Meteorological data for SDNWA was collected from the Global Water Institute climate tower installed at the site.

2.3. Water sampling and isotope analysis

Wetland pond water samples were collected every two weeks (and sometimes monthly) during the ice-free summer season (April–October) of 2014. Pond water samples were collected about 2 m from the bank at depths well below the pond water surface into the narrow mouth 50 mL Polypropylene (PP) bottles and sealed. Wetland pond temperature at various locations suggests that the pond water was well mixed. Rainfall samples were collected from dry-wet rain gauges that were filled with small amounts of paraffin oil to minimize evaporation of rainfall samples. The rain gauges were emptied in-between rain events. The location of the rain gauges is indicated in Fig. 1b. The amount and isotope compositions of precipitation from these gauges at the SDNWA were used for comparison with Saskatoon records. The amounts recorded during the period was used in 2014 model calculations.

All water samples were transported to the Stable Isotope Laboratory at the National Hydrology Research Centre, Saskatoon. The samples were left for debris to settle before stable isotopes analysis. The samples were then analyzed for $^{2}H/^{1}H$, and $^{18}O/^{16}O$ ratios using a Los Gatos Research DLT-100 liquid water isotope analyzer system coupled with a CTC LC-PAL liquid autosampler (Los Gatos Inc., California) following the procedures in Lis et al., (2008) and IAEA (2009). The isotope values are reported in the usual δ notation in ‰ vs. Vienna Standard Mean Ocean Water (VSMOW). Samples, standards and control samples (river water) were analyzed repeatedly six times, and the average value of the last four measurements was determined (IAEA, 2009). The internal

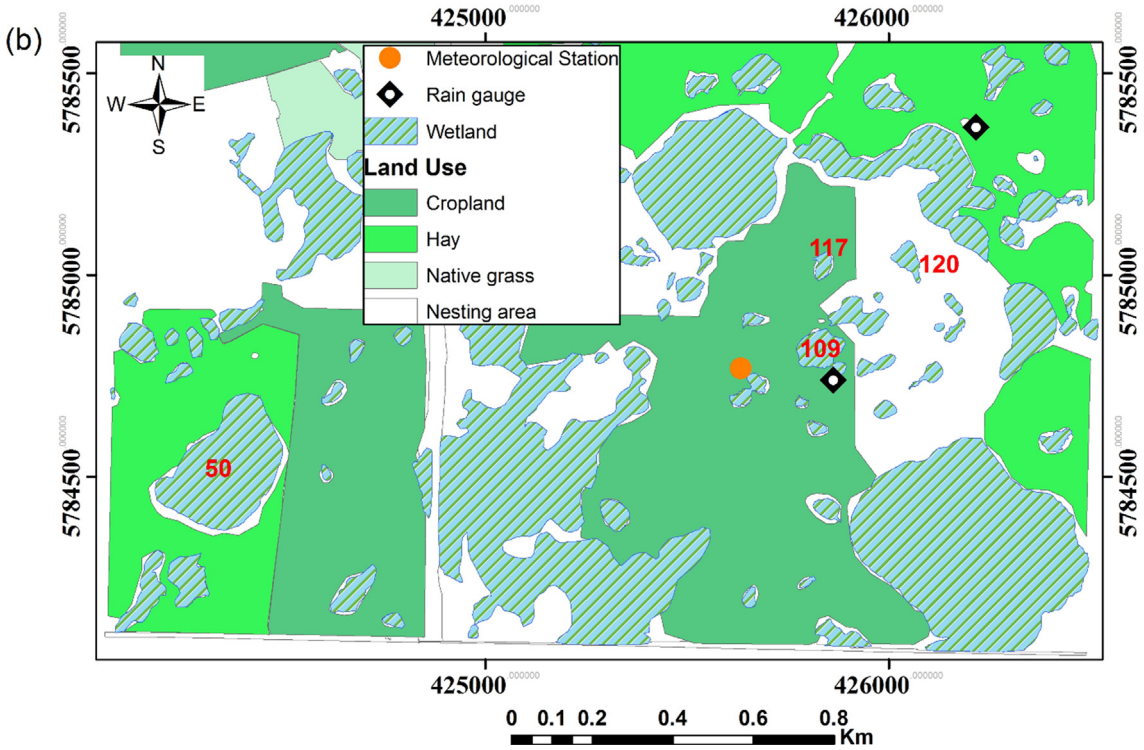

Fig. 1b. The St. Denis National Wildlife Area, Saskatchewan showing wetland in numbers used in this study and other wetlands and land use in the area.

laboratory standards INV1: $\delta^2H = -220.0‰$, $\delta^{18}O = -28.5‰$ and ROD3: $\delta^2H = -8.0‰$, $\delta^{18}O = -1.2‰$ were calibrated to the VSMOW2 and SLAP2 reference waters and used to normalize the results to the VSMOW-SLAP scale. The laboratory analytical precision is approximately ± 0.2‰ for $\delta^{18}O$, and ± 1.0‰ for δ^2H, respectively (Lis et al., 2008).

The stable isotope ratios of water collected between 1990 and 2007 (i.e., precipitation and pond samples) were analyzed using isotope-ratio mass spectrometers (IRMS). The protocols for the isotope-ratio mass spectrometer analysis follow the standard methods (Begley and Scrimgeour, 1997; Coleman et al., 1982; Eiler and Kitchen, 2001; Epstein and Mayeda, 1953; Karhu, 1997; Kelly et al., 2001; Socki, 1999). The water samples for oxygen isotope analysis were prepared by conventional H_2O–CO_2 equilibration (Epstein and Mayeda, 1953). About 5 mL of each sample was equilibrated with CO_2 gas at 25 ± 0.1 °C for 24 h. The CO_2 gas was cryogenically extracted and purified in a vacuum line. For deuterium analysis, Cr at 850 °C was used to produce hydrogen gas (Coleman et al., 1982). Both $^{18}O/^{16}O$ and $^2H/^1H$ ratios were determined relative to internal standards that were calibrated using Vienna-Standard Mean Ocean Water (V-SMOW). The data were normalized and reported in the delta notation (Coplen, 1988). The analytical reproducibility is ± 0.1‰ and ± 1.0‰ for $\delta^{18}O$ and δ^2H. Both offline dual-inlet (i.e., zinc reduction or uranium reduction) and continuous flow IRMS methods (i.e., Cr reduction or C reduction) have measurement accuracies of the order of (± 0.5 to ± 4‰) for δ^2H and the automated CF-IRMS methods such as C-reduction to CO and CO_2-H_2O equilibration were between ± 0.1 and ± 0.4‰ for $\delta^{18}O$ (Lis et al., 2008).

2.4. Archived data

Wetland pond water depths, water temperature, and isotope data, obtained from 1991 to 2016 and maintained by the National Hydrology Research Centre, Saskatoon was used to complement our data. Pond area, volume, and, shape factors obtained from the survey data of van der Kamp (2009, personal communication) and other relevant data found in published works (Hayashi et al., 2016; Hayashi and Van Der Kamp, 2000; Heagle et al., 2013; Heagle, 2008) were also employed in pond bathymetry evaluations. The precipitation records, relative humidity, and atmospheric temperature measurements of Saskatoon are available from Saskatchewan Research Council climate records (http://climate.weather.gc.ca/climateData/dailydata_e.html?StationID=47707). All the other data used in this study can be obtained from the Federated Research Data Repository at https://doi.org/10.20383/101.0115.

3. Wetland pond water and isotope mass balance model

3.1. Model development

The variables used in this model are given in Table 1.

The water balance equation for a wetland pond is given as:

$$\frac{dV}{dt} = A(P + J - O - E) \tag{3}$$

where A (m^2) is the area of open water of the pond, dV (m^3/d) is the change in volume of water in pond over the time period dt (d), P (m/d) is direct precipitation into the pond, J (m/d) is the lumped surface and subsurface inflow, O (m/d) is the lumped surface and subsurface outflow, and E (m/d) is the direct evaporation from the pond surface. The change in isotope mass in the pond is expressed as

$$\frac{d(V\delta)}{dt} = A(J\delta_J + P\delta_P - O\delta_o - E\delta_E) \tag{4}$$

where δ (‰) is the isotope composition ($\delta^{18}O$ or δ^2H) and subscripts relate to the water balance equation components defined above, and δ with no subscript refers to pond water.

Eqs. (3) and (4) can be applied to any surface water body. In general, inflow terms (i.e., surface run in and groundwater discharge), J, may carry isotopically distinct waters and hence modify the isotopic composition of the water body, outflow terms (i.e., spillage, soil infiltration, and plant transpiration), O, remove water without modifying the isotopic composition of the water body, and E removes water and

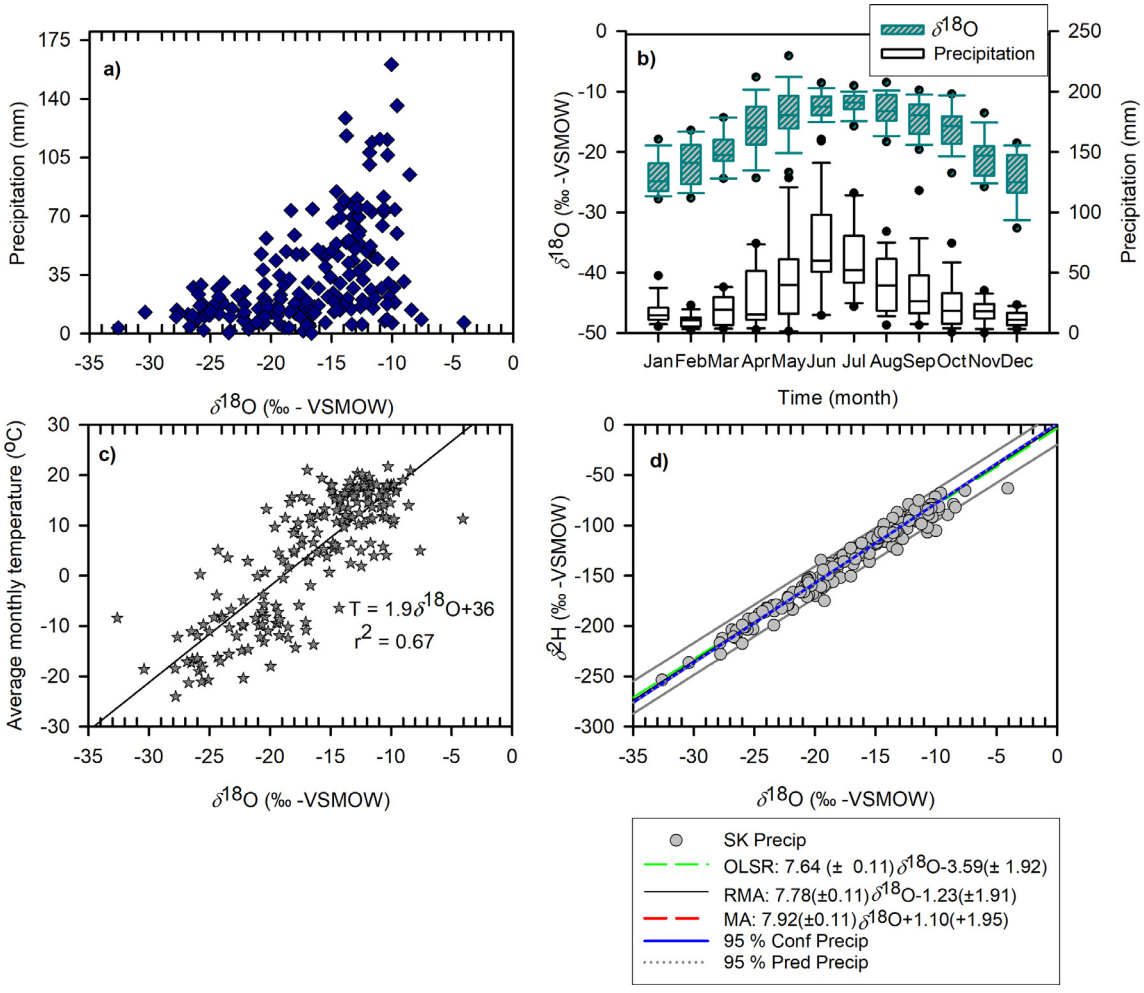

Fig. 2. Monthly Saskatoon precipitation June 1990–December 2014: (a) precipitation amount – $\delta^{18}O$; (b) $\delta^{18}O$ isotope (box up) and precipitation amount; (c) temperature – $\delta^{18}O$ and (d) local meteoric water lines (OLSR, RMA and MA) for Saskatoon. The $\delta^{2}H$ and $\delta^{18}O$ values of precipitation are in ‰, referenced to V-SMOW. The boxes in Fig. 2b mark the 25th–75th percentile range of data, whiskers mark the 10th–90th percentile range of data, and black horizontal lines mark the median.

modifies the isotopic composition of the remaining water in the pond. In small, well mixed, relatively shallow and seasonally dynamic ponds such as found in the North American Prairies during the ice-free summers, some simplifying assumptions about these terms can be made. We can assume that $J = 0$, and that water input into the pond is due only to rainfall on the pond, P. We can also assume that all the water loss as outflows, O, is infiltration, which subsequently goes to soil water, groundwater recharge, and transpiration. The justifications for these assumptions are stated below.

The primary input of water to the ponds, other than direct rainfall, comes from snowmelt runoff into the pond. For the period after the snow and ice melt, that the analysis of this paper is restricted to, the surface runoff processes that deliver water into the pond are ignored, and we use initial conditions based on the water levels and isotopic compositions caused by the snowmelt runoff. Heavy rainfall events can also cause surface runoff to occur, though these are historically fairly rare (Coles et al., 2017). In our dataset, there was one year (i.e., 2014) when this did happen, and in that case, the model was initialized after the rainfall-runoff event.

For ponds that receive a significant amount of water from groundwater input (that is discharge ponds as noted in Nachshon et al. (2013)), it would be necessary to estimate the amount of discharge water into the pond and the corresponding isotope composition of the groundwater, if this model will be applied to simulate water balance fluxes. That is a significant challenge worthy of further research, but not addressed here. In this study, we considered recharge ponds and therefore we do not include groundwater inflow.

Regarding pond outflows, it is not necessary to assume that soil infiltration and plant transpiration, termed here infiltration, is the only outflow, but we do so here because we know that the ponds selected did not spill during the period studied. A significant amount of the infiltration that occurs below ponds go to support riparian zone transpiration (Nachshon et al., 2013), with the remainder going to groundwater recharge and soil evaporation (Bam, 2018; Millar, 1971; Parsons et al., 2004). However, water lost to both riparian zone plant transpiration, soil, and groundwater recharge from the pond does not induce isotope fractionation in the pond water (Gibson and Edwards, 2002; Jasechko et al., 2013; Rothfuss et al., 2010; Yepez et al., 2003), and so that process has not been represented explicitly in this model. Thus, the infiltration reported is responsible for lateral seepage to transpiring marginal vegetation, soil evaporation and vertical seepage as groundwater recharge. To constrain each flux from the infiltration component, into transpiration, soil evaporation, and groundwater recharge, a coupled solute-isotope-water mass balance method (e.g., Dincer et al., 1979) or independent measurement of evapotranspiration at the site is required. At this stage, we did not attempt to distinguish how this flux, infiltration, is partitioned between groundwater recharge, soil evaporation, and plant transpiration fluxes even though it is a significant hydrological problem.

Substituting $J = 0$, and $\delta_o = \delta$ reduces Eqs. (3) and (4) to Eqs. (5)

Table 1
The list of variables used for calculation of evaporation and infiltration fluxes based on the Craig–Gordon model (Craig and Gordon, 1965) and equations from Gonfiantini (1986) and our isotope-water-mass balance model.

Variable	Description
A (m^2)	Area
E (m/d)	Evaporation rate
H (–)	Normalized relative humidity
J (m/d)	Inflow rate of overland runoff, rivers and groundwater
O(m/d)	Outflow rate of pond spillage and infiltration
β (–)	Basin profile parameter
P (m/d)	Precipitation rate over the pond
s (m^2)	Scale parameter
t (d)	Time
T (°C)	Temperature
V (m^3)	Volume of surface water stored
k (m)	Pond water depth
LEL	Local evaporation lines
δ_a (‰)	Delta of atmospheric water vapour
δ_E (‰)	Delta of evaporated water isotope composition
δ_i (‰)	The initial isotope composition of the pond
δ_t (‰)	The instantaneous isotope composition of the pond
δ_j (‰)	Delta of inflow water isotope composition
δ_p(‰)	Delta of rainfall isotope composition
δ_o (‰)	Delta of water outflow isotope composition
$\delta^{18}O$ (‰)	Delta of Oxygen-18 isotope composition
$\delta^{2}H$ (‰)	Delta of Hydrogen-2 isotope composition
ε	Total isotope fractionation factor (dependent on T and H)
α	Liquid-water vapour isotope fractionation factor (T dependent)
ϵ	Equilibrium isotope fractionation between liquid and vapour
$\Delta\epsilon$ (-)	The kinetic isotopic separation based on wind tunnel experiments (H dependent)
e_s (kPa)	Saturated vapour pressure over the pond
e_{sa} (kPa)	Saturated vapour pressure in air
e_{sw} (kPa)	Saturated vapour pressure near pond
n (–)	Surface roughness or smoothness constant
θ (–)	Advective term accounting for humidity buildup
C_k (%)	Kinetic isotope fractionation constant
x	Unknown quantity

and (6) respectively.

$$\frac{dV}{dt} = A(P - O - E) \tag{5}$$

$$V\frac{d\delta}{dt} + \delta\frac{dV}{dt} = A(P\delta_P - O\delta - E\delta_E) \tag{6}$$

Replacing dV/dt in Eq. (6) with Eq. (5) yields:

$$V\frac{d\delta}{dt} + \delta[A(P - O - E)] = A(P\delta_P - O\delta - E\delta_E) \tag{7}$$

which reduces to

$$\frac{d\delta}{dt} = \frac{A}{V}[P(\delta_P - \delta) - E(\delta_E - \delta)] \tag{8}$$

While the terms A, V, P, δ and δ_P can be measured directly in the field (or laboratory), E and δ_E cannot. The isotopic composition of moisture evaporating from the surface a lake, δ_E, is estimated by a linear resistance model of Craig and Gordon (1965) as defined (Gammons et al., 2006; Horita et al., 2008):

$$\delta_E = \frac{1}{1 - H + \frac{\Delta\epsilon}{1000}}\left(\frac{\delta - \epsilon}{\alpha} - H\delta_a - \frac{\Delta\epsilon}{1000}\right) \tag{9}$$

where ϵ (–) and $\Delta\epsilon$ are the equilibrium and kinetic isotopic separation between liquid and vapour, respectively, α (–) is the fractionation factor and H (–) is the relative humidity. The Craig and Gordon (1965) model was developed to describe the isotopic fractionation associated with evaporation. The model assumes the atmosphere above a given liquid surface to be three discrete layers: (i) a saturated sublayer with 100% relative humidity that attains isotopic equilibrium at the liquid-air interface; (ii) a laminar layer less than 100% relative humidity above the liquid-air surface (layer 1) where vertical transport of water molecule due to molecular diffusion across the humidity gradient results in isotopic fractionation; and (iii) a turbulent atmosphere where turbulent transport dominates with no isotopic fractionation.

The equilibrium isotopic separation between liquid and vapour, ϵ, is calculated as (Gonfiantini, 1986)

$$\epsilon = 1000(\alpha - 1 \tag{10}$$

where α is the fractionation factor which is a function of temperature, T (K). The equations of the liquid water-vapour fractionation factor (valid between 0 and 374 °C) were obtained from laboratory experiments and are given for $\delta^{18}O$ and $\delta^{2}H$ as follows (Horita and Wesolowski, 1994):

$$\ln\alpha_{18_O} \times 10^3 = -7.685 + 6.7123\left(\frac{10^3}{T}\right) - 1.6664\left(\frac{10^6}{T^2}\right) + 0.35041\left(\frac{10^9}{T^3}\right) \tag{11}$$

$$\ln\alpha_{2_H} \times 10^3 = 1158.8\left(\frac{T^3}{10^9}\right) - 1620.1\left(\frac{T^2}{10^6}\right) + 794.84\left(\frac{T}{10^3}\right) - 161.04 + 2.9992\left(\frac{10^9}{T^3}\right) \tag{12}$$

The equivalent kinetic isotopic separation based on wind tunnel experiments is calculated from (Araguas-Araguas et al., 2000):

$$\Delta\epsilon = (1 - H)\theta n C_k \tag{13}$$

where $n = 0.5$ for a rough surface, e.g., open water bodies and $n = 1$ for soil water, $\theta = (1 - H_o)(1 - H)$ is an advection term to account for the potential influence of humidity buildup, H_o is the adjusted humidity of the downwind atmosphere following admixture of evaporating moisture over the surface, often set to $\theta = 1$ for small water bodies, and C_k is the kinetic fractionation constant, which is 28.6% and 25.0% for oxygen-18 and deuterium, respectively. As a result, we have here

$$\Delta\epsilon_{18_O} = 14.2(1 - H) \tag{14}$$

$$\Delta\epsilon_{2_H} = 12.5(1 - H) \tag{15}$$

If the relative humidity, H, is measured near the pond/lake, it must be normalized to reflect the relative humidity over the pond surface under saturated conditions. The saturated vapour pressure, e_s (kPa), can be estimated from (Allen et al., 1998):

$$e_s = 0.6108\mathrm{e}^{\left[\frac{17.27(T-273)}{T}\right]} \tag{16}$$

where T (Kelvin) is the temperature measured near the pond. The normalized relative humidity, H is calculated from the ratio of e_s in air (e_{sa}) and e_s in water (e_{sw}) based on temperature measurements and multiplied by the relative humidity measured near the pond/lake.

The ambient atmospheric water vapour isotope composition, δ_a, can be measured directly, estimated from precipitation values, or calculated from local evaporation lines of surface water within the catchment (Clark and Fritz, 1997; Gammons et al., 2006; Gibson and Reid, 2014; Jacob and Sonntag, 1991; Skrzypek et al., 2015). The ambient atmospheric water vapour isotope compositions (δ_a) used here were calculated using the local evaporation lines (Section 3.2) of each ponds in a given year.

Now substituting Eq. (9), the equation for estimating the isotopic composition of the evaporating water, into the isotope-water-mass balance equation (Eq. (8)) yields:

$$\frac{d\delta}{dt} = \frac{A}{V}\left[P(\delta_p - \delta) - \frac{E}{1 - H + [\frac{\Delta\epsilon}{1000}]}\left(\frac{\delta - \epsilon}{\alpha} - H\delta_a - \frac{\Delta\epsilon}{1000}\right) - E\delta)\right] \tag{17}$$

factorizing and re-arranging, gives

$$\frac{d\delta}{dt} = \frac{A}{V}[P(\delta_p - \delta) + E(B - C\delta)] \tag{18}$$

where

$$B = \frac{H\delta_a + \frac{\Delta\epsilon}{1000} + \frac{\epsilon}{\alpha}}{1 - H + \left[\frac{\Delta\epsilon}{1000}\right]} \tag{19}$$

and

$$C = \frac{H - \left[\frac{\Delta\epsilon}{1000}\right] - \frac{\epsilon}{1000\alpha}}{1 - H + \left[\frac{\Delta\epsilon}{1000}\right]} \tag{20}$$

Integrating Eq. (18) with respect to the isotope composition of the pond water, δ, and time, t gives:

$$\delta_t = \delta_i e^{-\frac{(AP+AEC)t}{V}} + \frac{EB + P\delta_p}{P + EC}\left(1 - e^{-\frac{(AP+AEC)t}{V}}\right) \tag{21}$$

δ_i refers to the initial isotopic composition of the pond.

Estimating the water balance using the wetland pond water level, we substituted Eqs. (1) and (2) into Eq. (5) resulting in

$$\frac{d}{dt}\left[\frac{sk^{1+\frac{2}{\beta}}}{(1+\frac{2}{\beta})}\right] * \frac{1}{sk^{2/\beta}} = (P - O - E) \tag{22}$$

Integrating with respect to t and factorizing we have:

$$k_t = k_i + \sqrt{\frac{P(t) - O(t) - E(t)}{2(\frac{2}{\beta} + 1)}} \tag{23}$$

k_i refers to the initial water level of the pond.

Eqs. (23) and (21) solve the water balance and isotope-water-mass balance, respectively. The water balance equation simulates the pond water level, given some specified total water loss from the pond (E and O combined). Thus, given observations of pond levels, inverse modelling can be used to identify the total loss, i.e., $E + O$, but not the partitioning between these variables. Similarly, the isotope – water-mass model takes some specified E to simulate the pond isotope composition. Given observations of the pond isotope composition, inverse modelling can be used to identify E, and hence O. Inverse modelling was achieved here by optimization, minimizing the root mean squared error, RMSE, of pond level (stage 1) or pond isotopic composition (stage 2), by changing $E + O$ (stage 1) and E (stage 2). Optimization was performed in Python 2.7 using the Scipy function fmin, which uses a Nelder-Mead simplex algorithm (https://docs.scipy.org/doc/scipy/reference/generated/scipy.optimize.fmin.html).

This model can be used to *i)* estimate E and O from a specific pond from past observations of pond/climate variables, or to *ii)* project pond isotope compositions into the future, given some prescribed partitioning of E and O, along with projections of the hydrometeorological variables. The model scripts are attached as Supplementary material (S1) in the Appendix. This script was written and run in Python 2.7.2 (Python Software Foundation, US, 2011), and reads input data from Microsoft Excel files. The code and all the data set can be found at https://github.com/amireson/PrairiePondModel.

3.2. Stable isotope composition of ambient atmospheric water vapour

The isotope composition of ambient atmospheric water vapour, δ_a, can be measured directly, estimated from precipitation values, or calculated from local evaporation lines of surface water within the catchment (Clark and Fritz, 1997; Gammons et al., 2006; Gibson and Reid, 2014; Jacob and Sonntag, 1991; Skrzypek et al., 2015). Here δ_a was computed using the pond evaporation lines (LEL, Table 2) obtained from the multiple measurements of the isotopic changes within each individual wetland pond (Bennett et al., 2008; Gibson et al., 2008a,b, 2016; Gibson and Reid, 2014; Skrzypek et al., 2015). Because the isotopic compositions of pond water in the prairie environment is strongly influenced by seasonal climatic effects (i.e., Figs. 3 and 4) resulting in highly seasonal evaporation rates, the ambient atmospheric water vapour is calculated assuming the atmosphere is in equilibrium with precipitation during the evaporation season (Gibson, 2002a,b, 2016). Thus, an effective precipitation-vapour separation ($\in$ effective, Gibson et al., 2016) is assumed where the evaporation line slope and the effective isotopic separation between amount-weighted precipitation (falling near the intersection of local evaporation line and meteoric water line) and the evaporation-flux weighted moisture is less than the equilibrium separation. The δ_a was estimated from local records of the spring-summer rainfall stable isotope composition (δ_P) as follows (Bennett et al., 2008; Gibson et al., 2016; Gibson and Reid, 2014; Skrzypek et al., 2015):

$$\delta_a = (\delta_P - x\in)/(1 - x \in /1000) \tag{24}$$

where (δ_P) is the stable isotope composition of rain (δ^2H and $\delta^{18}O$) and $\in$ is the equilibrium isotopic separation between liquid and vapour; which depends only on temperature as described in Eqs. (10)–(12) (Horita and Wesolowski, 1994). Initially, Eq. (24) was solved using $x = 1.0$ and then the slope of LEL was calculated from Eq. (25):

$$\text{Slope}_{(\text{LEL})} = \frac{\left[\frac{H*\left(\frac{\delta^2_{Ha} - \delta^2_{HP}}{1000}\right) + \frac{\varepsilon}{1000}*\left(1 + \frac{\delta^2_{HP}}{1000}\right)}{H - \frac{\varepsilon}{1000}}\right]H}{\left[\frac{\boldsymbol{H*\left(\frac{\delta^{18}_{Oa} - \delta^{18}_{OP}}{1000}\right)} + \frac{\varepsilon}{1000}*\left(1 + \frac{\delta^{18}_{OP}}{1000}\right)}{\boldsymbol{H} - \frac{\varepsilon}{1000}}\right]\boldsymbol{O}} \tag{25}$$

where H is air relative humidity (given as a fraction), ε is the total fractionation factor and equals the sum of the equilibrium isotope fractionation factor $\in$, as given above plus the kinetic isotope fractionation factor $\Delta\in$ (Gibson and Reid, 2010):

$$\varepsilon = \frac{\epsilon}{\alpha} + \Delta\in \tag{26}$$

The calculation was then repeated a number of times using x between 1.0 and 0.1. The final δ_a values were selected from the x parameter that gave the lowest difference between the calculated slope of LEL (Eq. (25)) and the observed slope of LEL obtained from field measurements (in this case x reached the boundary values between 0.6 and 1.0). The slope of LEL and the final δ_a values for the ponds (Table 2) were generally within the range of values reported from the global basis analysis of the International Atomic Energy Agency's Global Network for Isotopes in Precipitation database (Gibson et al., 2008a,b).

3.3. Sensitivity analyses

Sensitivity tests were run to determine the effects of variations in the climatic variables (i.e., relative humidity, H, atmospheric vapour composition, δa, precipitation, P and temperature, T), and pond bathymetry parameters (i.e., s and β), on the modeled pond isotope composition, δ_t. Sensitivity simulations were conducted on a monthly time step for the 2014 model year for Pond 109. A univariate sensitivity analysis was performed using baseline pond parameters and average values of the climatic parameters obtained from the site. The effect of each parameter on the model was tested one at a time by increasing and decreasing the parameters to a high and low value. The parameters were varied by some percentage margins based on the approximate range of values that can be measured in the region. The model sensitivity to the variations in each parameter was tested between the period of 22nd May and 16th September 2014. For the sensitivity analyses, $E + O$ (the total water outflow) was fixed at an arbitrary value that ensured a reasonable water balance, and the ratio $E/(E + O)$ (i.e., evaporation to total water outflow) was varied from 0.1 (i.e.,

Table 2
Summary of average climate, isotopic and basin bathymetry parameters of ponds and pond evaporation slopes, m tested using the Prairie wetland isotope-water mass balance model at St Denis National Wildlife Area, Saskatchewan.

Pond	Year	Precipitation			Atmospheric parameters				Shape parameters		Slope of LEL (–)
		Amount (mm)	$\delta^{18}O_p$ (‰)	$\delta^{2}H_p$ (‰)	T (°C)	H (–)	$\delta^{18}O_a$ (‰)	$\delta^{2}H_a$ (‰)	s (m^2)	β (–)	
50	1994	173	−11.9	−96.4	15.4	0.68	−19.7	−155.6	29,500	2.5	5.4
50	1998	84	−11.7	−96.9	16.9	0.63	−20.4	−161.7	29,500	2.5	5.3
50	1999	150	−13.0	−107.2	16.4	0.61	−22.7	−171.95	29,500	2.5	5.3
50	2014	67	−13.2	−107.2	14.8	0.70	−23.1	−179.7	29,500	2.5	5.8
109	1994	157	−12.5	−103.0	15.4	0.68	−19.4	−154.8	3180	1.6	5.9
109	1997	118	−13.3	−102.3	16.8	0.66	−22.0	−166.8	3180	1.6	5.2
109	1998	108	−11.7	−96.9	16.9	0.63	−20.4	−161.7	3180	1.6	5.4
109	2014	108	−13.5	−103.7	11.2	0.68	−23.7	−179.9	3180	1.6	5.6
117	2014	88	−13.1	−104.6	11.9	0.70	−21.2	−166.0	2844	1.0	5.9
120	2014	165	−13.3	−103.3	11.2	0.70	−23.5	−179.5	2798	2.7	5.7

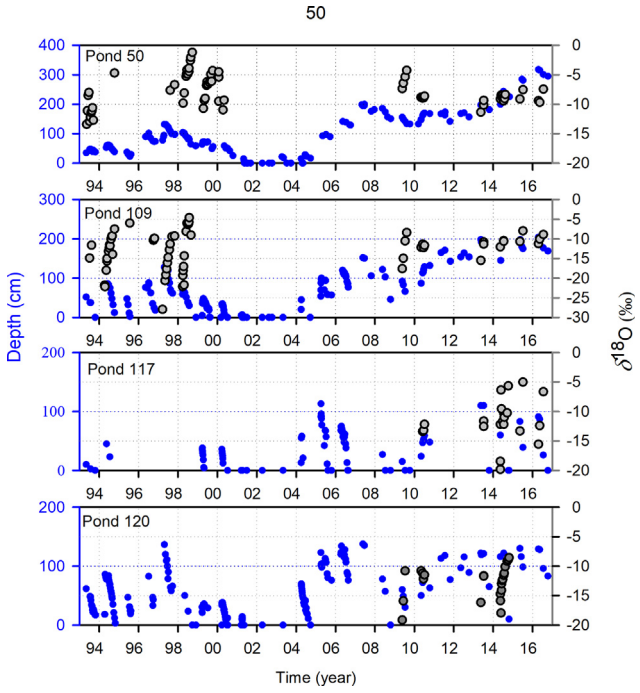

Fig. 3. Yearly seasonal variations in pond depth and isotope compositions for wetland 50, 109, 117, and 120 from 1993 to 2016 at the St. Denis Wildlife National Area, Saskatchewan.

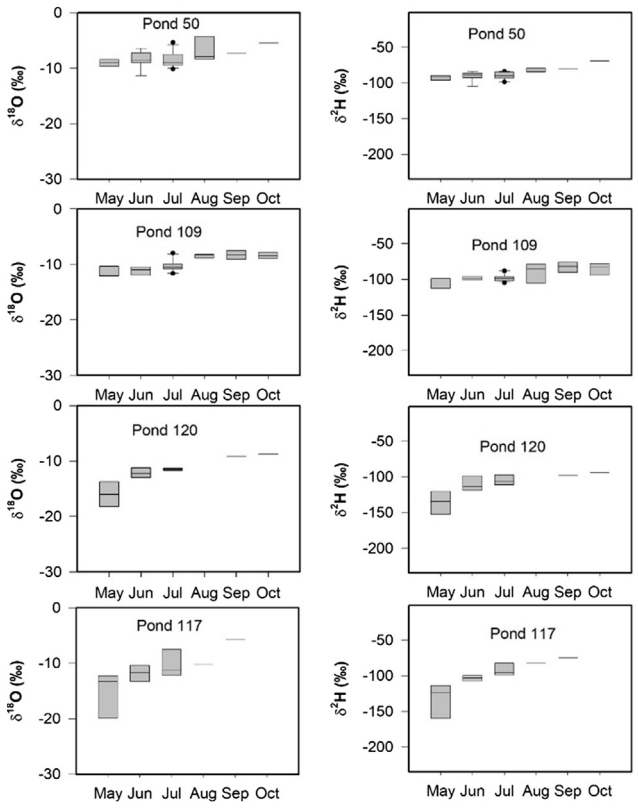

Fig. 4. Monthly time series of pond isotope evolution within and between ponds for the period between May and October from 2010 to 2016.

infiltration dominates) to 0.9 (i.e., evaporation dominates).

3.4. Model application to SDNWA

The model was applied to estimate E and O for four ponds at the SDNWA, one ephemeral (pond 117), one semi-permanent (pond 120), and two permanent (pond 50 and 109). The model driving data is given in Table 2. Since the model assumes there is no input to the pond, other than from direct rainfall, it was be initiated after snowmelt, or any major rainfall-runoff into the pond. The initial conditions for the model are the water level and the isotopic composition of the pond water. The start and end date for each simulation (i.e., for each pond and each year) was chosen based on the periods where there were minimal surface runoff into the pond during the summer. The simulated years (1994, 1997, 1998, 1999 and 2014) were the years for which pond water levels, isotope and climate data were available.

Table 2. Summary of average climate parameters, isotopic and basin bathymetry of ponds tested using the new water and isotope-water mass balance model at St. Denis National Wildlife Area, Saskatchewan. The δ represent average isotope compositions of precipitation and ambient atmospheric moisture. s and β are the pond bathymetric parameters used in Eqs. (1) and (2).

3.5. Model comparison with existing Craig-Gordon based models

An existing model for estimating the evaporative loss of water from a surface water body using stable isotopes is available through the *Hydrocalculator* software (Skrzypek et al., 2015). The software is a compilation of the existing isotope-water mass balance models that employed the Craig and Gordon (1965) model to compute the isotope composition of the vapour from the surface of an evaporating water body. These isotope-water-mass balance models are available in two formulations: i) the steady-state configuration (hereafter the HCSS model), which aims to look at the long-term response of a water body under steady-conditions, where the inflow equals the outflow, and there is no change in storage; and ii) the non-steady-state configuration (hereafter the HCNS model). The HCSS model aims to look at the long-

term response of a water body under steady-conditions, where the inflow equals the outflow, and there is no change in storage. The HCNS model aims to look at the short-term response of a water body when there is a change in storage, but the only loss term is due to evaporation. The primary advantage of these models over our model is that much less observational data are required, and it is, therefore, useful to get estimates of evaporation from large water bodies in data scarce areas. However, for small prairie ponds, the assumptions are not appropriate – the isotopic composition of the precipitation has an enormous impact on the pond isotope composition, the pond storage changes are highly significant, with ponds often wholly emptying, and the water loses are due to infiltration as well as evaporation. None-theless, we aimed to compare the average evaporation estimates from these two models, HCSS and HCNS, with our estimates, to see how appropriate these simpler approaches are for small dynamic prairie ponds. We note here average estimates from the *Hydrocalculator* software because the output of evaporation ratios are based on the single isotope (i.e., $\delta^{18}O$ and $\delta^{2}H$).

4. Results

4.1. Stable isotope characteristics of prairie wetlands

Fig. 3 shows the temporal variation in stable isotope compositions and pond depth as monitored in Prairie wetlands from 1993 to 2016 (spring-fall seasons). The water level is at its maximum after snowmelt, when the isotopic enrichment is minimum. Throughout the summer water levels drop via a combination of evapotranspiration and infiltration; isotopic enrichment develops progressively in response to evaporation. Fig. 4 shows continuous $\delta^{18}O$ and $\delta^{2}H$ enrichment in of the ponds between the years 2010 to 2016. Fig. 4 also shows gradual enrichment in the water isotope compositions of $\delta^{18}O$ and $\delta^{2}H$ with time and within the ponds from the spring (May) to the fall (September). The water stable isotope compositions found in the permanent ponds (50 and 109) are generally enriched even at the start of the season (that is the onset of the spring season). Fig. 5 shows a scatter plot of pond isotope values to examine the effect of evaporation on the wetland ponds for four wetland ponds 50, 109, 117 and 120 at the St Denis National Wildlife Area. The pond isotope values fall below the Saskatoon local meteoric water line defining local evaporation lines slopes between 5.2 and 6.4.

4.2. Model sensitivity

The results of the sensitivity tests are shown in Fig. 6 as contour plots of how the isotope compositions of the pond water change as we impose changes in the relative proportion of evaporation to total pond losses (i.e., evaporation plus infiltration), and with perturbation to the parameter values. The baseline condition (i.e., the center column in each of the subplots) shows how the pond isotope composition is progressively enriched as the proportion of evaporation increases. The parametric perturbations are shown in the left and right columns in the same subplots, and the more sensitive a parameter is, the more these contours deviate from the baseline contour. The contours in Fig. 6 suggest that the model is highly sensitive to both relative humidity and atmospheric water vapour isotope composition. Both of these parameters will have a significant impact on surface water hydrological flux estimates and pond isotope compositions. The effect of precipitation additions and temperature are similarly sensitive when the values of these parameters are estimated close to 50% of the original values. The model is also moderately sensitive to changing pond basin profile, β, but relatively insensitive to pond scale parameter, s. These observations are similar to those reported in earlier studies (Gammons et al., 2006; Gat, 1995; Gibson et al., 1993; Gibson, 2002a,b; Gonfiantini, 1986; Steinman et al., 2010). Minimizing errors in measurement of the sensitive parameters and assumptions about how these parameters vary with time will reduce uncertainty and improve model outputs.

4.3. Model application to SDNWA

The comparative results for model outputs and field observations are shown for the permanent ponds (50 and 109), the semi-permanent pond (120), and ephemeral pond (117) respectively in Fig. 7. The root means squared error (RMSE) values for simulated model outputs and field observed data ranged between 0.00 and 0.29 m for pond water levels and 0.02 and 0.10‰ for isotope composition values in all ponds.

Table 3 shows the water balance and the estimated partitioned fluxes of open-water evaporation and infiltration. Pond 109, a permanent recharge pond, has infiltration rates between 2.3 and 4.8 mm/d and evaporation rates of between 0.74 and 1.6 mm/d. The ratio of evaporation loss to total water loss, $E/(E + O)$, ranges from 13% to 40% (mean of 30%) which shows that infiltration is the dominant loss, on average accounting for approximately two thirds of the total loss. Pond 50, also a permanent pond, but not a recharge pond, has infiltration rates of between 0.99 and 1.3 mm/d and evaporation rates between 0.97 and 2.8 mm/d. Evaporation losses account for 43%–74% (mean of 60%) of all water losses from pond 50, and evaporation is therefore the dominant loss, on average accounting for approximately two thirds of the total water loss. Infiltration rates under the ephemeral Pond 117 and the semi-permanent pond 120 were 9.2 and to 5.8 mm/d, respectively, markedly higher than the permanent ponds in 2014 when isotope values and water levels in all ponds were measured. Evaporation rates in 2014 from ponds 117 and 120 were of a similar magnitude, at 0.88 and 1.2 mm/d, respectively. In the ponds 117 and 120, infiltration strongly dominate the water balance, accounting for 91% and 83% of water loses, respectively.

4.4. Model comparison with the existing Craig-Gordon based models

The HCSS model assumes steady-state conditions in the pond (inflow equals total outflow, no change in storage) and the model outputs the fraction of evaporation over inflow, E/I. The HCNS model assumes transient conditions (storage drops over time) and the only loss is due to evaporation, and the model outputs the fraction of evaporation to initial storage, E/k_i. We used the *Hydrocalculator* software to output these fractions separately for $\delta^{18}O$ and $\delta^{2}H$ data (data used are provided in Supplementary material S2, and Table 2) for both models. The average fractions were then used to calculated average E values for each model. Table 4 shows the evaporation rates estimated by the HCSS, HCNS and our model.

5. Discussion

5.1. Stable isotope characteristics of prairie wetlands

In the Canadian prairies, wetland ponds accumulate substantial amounts of snowfall and snowmelt runoff water during the winter and spring melt seasons. They tend to lose this water to evaporation and infiltration during the summer period. The result of course is the regular seasonal variations in water levels as shown (Fig. 3). The stable isotope compositions of ponds also follow predictable seasonal patterns: in spring the pond water is depleted due to additions of isotopically light snowmelt, and through the summer months the waters are progressively enriched by evaporation (Fig. 4).

We found that $\delta^{18}O$ and $\delta^{2}H$ in the permanent ponds were generally more enriched and less variable compared with the isotope composition of the semi-permanent and ephemeral ponds at the start of the spring season. We attribute the more positive values of $\delta^{18}O$ and $\delta^{2}H$ in the permanent ponds to the presence of large volumes of evaporated water retained from the previous year(s). Snowmelt $\delta^{18}O$ and $\delta^{2}H$ signatures are more negative than the residual evaporated pond water from previous years. The mixing of the residual evaporated waters with the

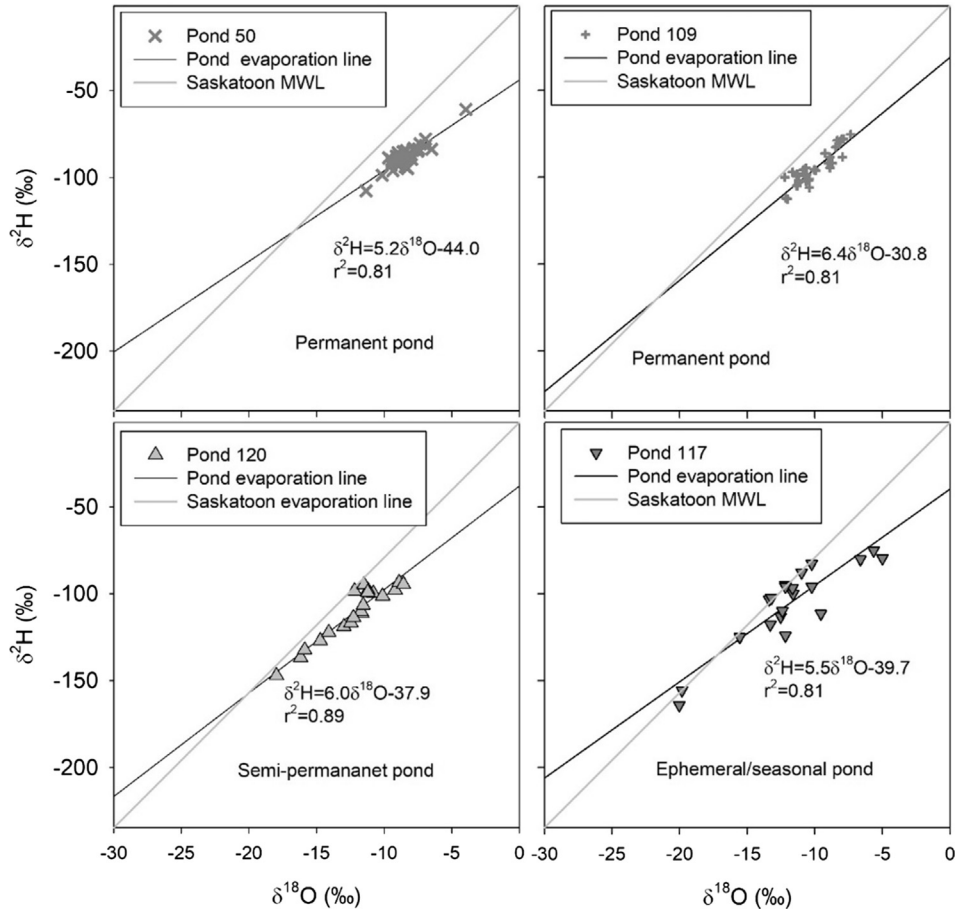

Fig. 5. Scatter plot of δ^2H-δ^{18}O of ponds with Saskatoon Local Meteoric Water Line (SKLMWL) for May–October of 2010–2016 at St Denis Wildlife National Area, Saskatchewan. Pond isotopes show deviation from SKLMWL indicating evaporitic behavior.

snowmelt water of the spring season results in the enriched δ^{18}O and δ^2H signals found in the large and permanent ponds at the start of the season (spring). This is different to the isotopic composition in the semi-permanent and ephemeral ponds where little or no evaporated water is retained from the previous season. Consequently, light snowmelt water serves as the initial water source for the ephemeral ponds and as a result, these ponds generally show more negative δ^{18}O and δ^2H compositions. These differences in the early spring isotope compositions observed in different pond types suggests that the seasonal δ^{18}O and δ^2H isotope compositions could be used to distinguish the hydrologic process behaviour in this region.

Between May to late October (Fig. 4), there was consistent, progressive enrichment in δ^{18}O and δ^2H for all ponds, due to evaporation in the pond. This evaporation effect is reflected in the lower slopes in dual isotope space for the pond evaporation lines (Fig. 5). The lower slopes of these evaporation lines (compared to the local meteoric water line) is as a result of kinetic fractionation induced by the evaporation process in an environment of relatively low humidity (Clark and Fritz, 1997; Gammons et al., 2006). We hypothesize that the differences in the slopes of the local evaporation lines of the ponds (Table 2) are as a result of several factors: vegetation cover around the pond, evaporation rate from the ponds, the volume of water and isotope composition of water stored from previous years, and whether or not the pond is losing or gain water to groundwater.

5.2. Model performance and sensitivity

The RMSE values for simulated model outputs and field observed data suggests that the performance of the model is reasonable for simulating both isotope compositions and water levels. The errors are generally of a similar in magnitude to the lowest analytical precision for δ^{18}O and δ^2H measurements, which is ± 0.2‰ and ± 1.0‰, respectively (Lis et al., 2008), and the observational accuracy in determining maximum water depth from ponds, which are mostly within 50 mm (Conly et al., 2004).

The comparison of water balance components between different types of wetland ponds shows that infiltration rates are highest in the ephemeral/semi-permanent pond (117 and 120), lower in the permanent recharge pond (pond 109) and lowest in the largest permanent pond (pond 50). The observation is consistent with our understanding of how these ponds function in the landscape (Stewart and Kantrud, 1971; Hayashi et al., 1998; van der Kamp and Hayashi, 2009; Heagle et al., 2013). The relatively high evaporation rate from the larger pond (Pond 50) is attributed to the larger surface area, and the relatively high exposure of the pond to wind and radiation, compared with the more sheltered recharge pond 109.

The model is most strongly affected by changes in relative humidity of the free vapour, H (Fig. 6a). With ± 15% changes in H, a considerable difference can be seen between the isotope compositions of the remaining pond water and the baseline isotope composition. The influence of H on kinetic fractionation process that occurs during evaporation of water vapour from surface water bodies are noted in Eqs. (9), (13), (19) and (25). This influence is directly related to the changes in the pond evaporation lines and hence the ambient atmospheric water vapour composition and the final hydrologic balance of the pond. Decreasing the relative humidity by 15% results in more enrichment of the isotopic composition of the remaining pond water.

The atmospheric water vapour isotopic composition, δ_a also exerts a

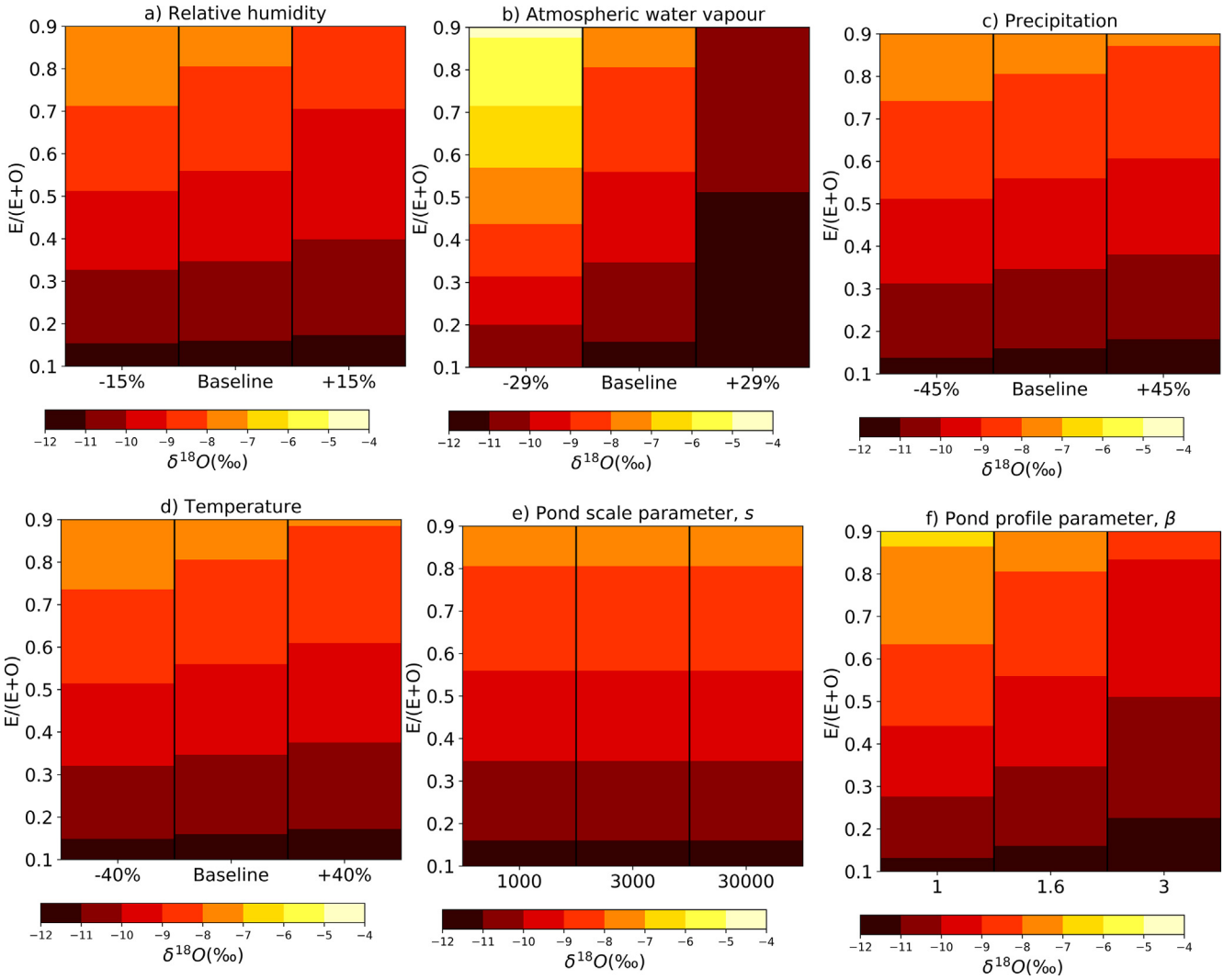

Fig. 6. Contour plot showing the sensitivity of pond isotopic composition, $\delta^{18}O$, to climate and pond geometry parameters.

strong impact on the model (although to a lesser degree than H. Changes in surface water isotope composition are driven by turbulent/diffusion mass transfer mechanisms and humidity (Eqs. (9), (17) and (25)). Kinetic fractionation during non-equilibrium evaporation of water as the result of the enhanced diffusion of the lighter isotope ($^1H_2{}^{16}O$) relative to heavier isotopologues ($^1H^2H^{16}O$ and $^1H_2{}^{18}O$) from the boundary layer to the open air (Clark, 2015; Gat, 2008). Field observations and laboratory experiments (Craig et al., 1963; Gat, 1995; Kumar and Nachiappan, 1999) have shown that an isotopic build-up will continue until the difference between the isotopic composition of the water body and that of its evaporate reaches isotopic equilibrium. Equilibrium isotopic conditions are unlikely in the field, as wind continuously replaces the air above the pond. This means that the ambient atmospheric isotope composition has a strong impact on the estimated hydrological fluxes. Future work should focus on more accurate ways of evaluating this variable.

Precipitation, P, was moderately sensitive in controlling differences in the pond isotopic composition as a simple function of dilution or mixing (as seen in Eq. (21)). Temperature, T, was also moderately sensitive. T influences evaporation rates and Fig. 6 shows that this is due to the direct control of T on the liquid-vapour equilibrium fractionation factor for evaporating water (Eqs. (11) and (12)). The impact of precipitation amount and temperature on the isotope composition of the remaining pond water is unsurprising. And the effect of temperature on the isotope composition of lake water and precipitation in the mid- and high latitude regions is well documented (Dansgard, 1964; Gat, 1996; Rozanski et al., 1992). Air temperature also influences evaporation, however, there are potential feedbacks that complicate such influence. For example, evaporation from an large lake or transpiration from the riparian vegetation around the pond may suppress air temperature and reduce pond evaporative losses. Alternatively, a smaller pond at the same temperature, may see increased evaporation with less vegetation cover (Mohammed and Tarboton, 2011).

The pond scale parameter, s, determines the overall size of the pond surface area, as a function of pond depth, and is a relatively insensitive parameter. Conversely, the pond profile parameter, β, which determines the form of the relationship between area and depth is highly sensitive. The insensitivity of the pond scale parameter, s, which determines the overall size of the pond surface area as a function of pond depth is not surprising because the substitution of the expressions for A and V (Eqs. (1) and (2)) into Eq. (8), cancels s out. Conversely, the highly sensitive nature of the pond profile parameter, β, suggests the shape of the ponds (area, depth, and volume) is essential for estimating flux losses. It follows, therefore, that the simplifying assumption that the pond area remains fixed as the depth changes are unsuitable for relatively small ponds as considered in this study.

The isotope-mass-balance model is most sensitive to controls of relative humidity, atmospheric water vapour isotope composition and pond shape, roughly in that order. These factors are followed by precipitation amount, temperature, and pond scale. Reducing the errors in

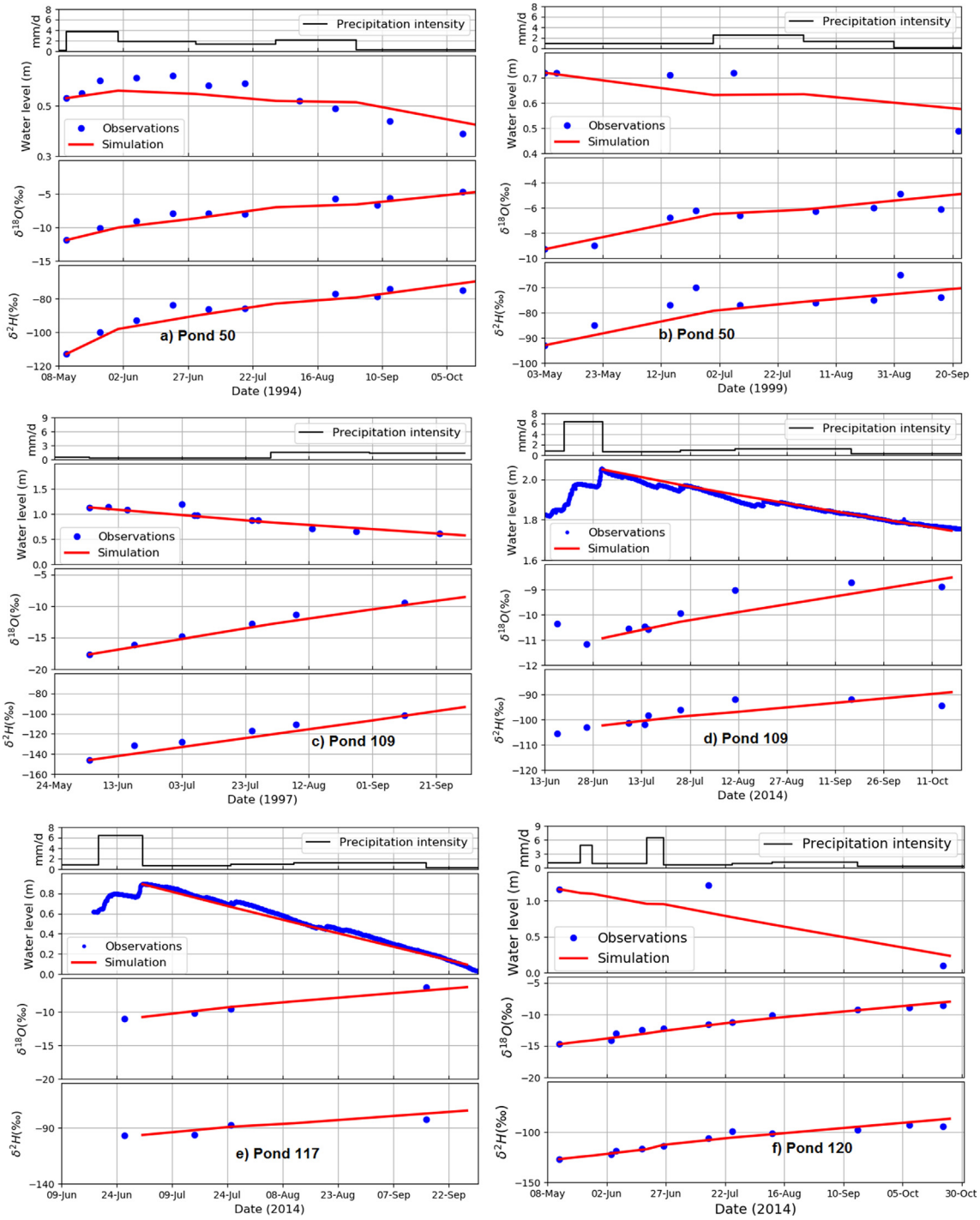

Fig. 7. Model performance compared with field observations of water level, $\delta^{18}O$ and $\delta^{2}H$ for some selected years 1994, 1997, 1999 and 2014 for which all required field observations were available for pond 117, 120, 109 and 50.

measurement of the most sensitive parameters and applying the correct assumptions about how these parameters vary with time will improve this model.

5.3. Comparison with field observations

The pond infiltration rates vary from 0.9 to 9.2 mm/d between years and between ponds. These infiltration rates are comparable to Darcy flux calculations of 0.83–1.38 mm/d by Woo and Rowsell (1993) and residual curve flux estimate by Hayashi et al. (1998) for SDNWA on the order of 9.4 mm/d. Work by Parsons et al (2004) in 1999 used tracer-mass balance estimates to calculate infiltration and found flux rates in the range 1.7–4.5 mm/d. The variability in these infiltration estimates can be likely explained by 3 factors: (1) pond type (i.e., ephemeral/temporal, or semi-permanent, or permanent), (2) antecedent moisture content of the substrate beneath the wetland pond before snowmelt, and (3) the meteorological conditions during the melt period (Granger et al., 1984; Hayashi et al., 2016). Studies have shown that infiltration rates under ephemeral and temporal ponds are higher than permanent ponds (Hayashi et al., 2016; Johnson et al., 2010; Parsons et al., 2004; Waiser, 2006; Winter and Rosenberry, 1998).

The pond infiltration rates and proportions of the total water loss

Table 3
Simulation results for all ponds and all years. RMSEs are the sums of these δ and water level calculated for $\delta^{18}O$ and $\delta^{2}H$ and water levels during the modelling period.

Pond		50				109				117	120
Year		1994	1998	1999	2014	1994	1997	1998	2014	2014	2014
No. of days		173	84	150	67	157	118	108	108	88	165
Initial $\boldsymbol{A}$ m^2		17,735	26,365	22,661	74,762	2410	3701	1927	7756	2261	3124
Final $\boldsymbol{A}$ m^2		14,039	20,504	18,746	71,296	585	1594	702	6353	25	984
Initial $\boldsymbol{h}$ (m)		0.53	0.87	0.72	3.20	0.80	1.13	0.67	2.05	0.89	1.16
Final $\boldsymbol{h}$ (m)		0.40	0.64	0.57	3.02	0.26	0.57	0.30	1.75	0.09	0.23
$\Delta \boldsymbol{S}$ (mm)		134	235	152	184	544	556	372	304	799	927
$\boldsymbol{P}$	mm	254	95	222	66	328	105	70	108	85	218
	mm/d	1.47	1.13	1.48	0.99	2.09	0.89	0.65	1.00	0.97	1.32
$\boldsymbol{E}$	mm	168	226	207	184	117	167	173	166	77	191
	mm/d	0.97	2.69	1.38	2.75	0.74	1.42	1.60	1.54	0.88	1.16
$\boldsymbol{I}$	mm	220	103	167	66	755	494	269	247	807	955
	mm/d	1.27	1.23	1.11	0.99	4.81	4.19	2.49	2.28	9.17	5.79
$E/(E+I)$		43%	69%	55%	74%	13%	25%	39%	40%	9%	17%
RMSE δ (‰)		0.11	0.18	0.06	0.09	0.06	0.09	0.12	0.09	0.05	0.07
RMSE $\boldsymbol{h}$ (m)		0.03	0.01	0.05	0.01	0.12	0.04	0.00	0.02	0.02	0.24

estimated using our model compared well with estimates obtained in previous hydrological studies at Pond 109 at the SDNWA. Parsons et al., (2004) showed for Pond 109 using an artificial bromide tracer, that the daily infiltration rate was 1.7 mm/day in May and 4.5 mm/d between June and July. These infiltration rates accounted for 47% and 67% of total pond water-loss in May and June/July, respectively. The average infiltration value of 3.9 mm/d compares remarkably well with our independent, model-based estimate of 3.4 mm/d for Pond 109. The daily open-water evaporation rates for Pond 109 measured for the same period were 1.9 mm/d in May and 2.2 mm/d for June and July (Parsons et al., 2004). Our estimate of 1.33 mm/d was somewhat lower than their average value. Hayashi et al. (1998) reported open water evaporation rates of ~3 mm/d for a two week period in 1995 for Pond 109 based on Bowen ratio energy balance and evaporation pan measurements.

5.4. Our model in comparison to other models

Table 4 shows the modeled estimates of evaporation, E, from our model, the HCNS model and the *Hydrocalculator*. While these rates vary considerably, it is perhaps not surprising given that the three models have different assumptions and are designed to answer different questions.

The HCNS model does not partition E and O, since O is assumed to be zero. As a result, HCNS showed no differences in rates of evaporation-inflow ratios between the different types of ponds and overestimated the evaporation fraction for all ponds (Table 4). HCNS is therefore poorly suited for obtaining reliable surface water fluxes in small prairie ponds that lose water and receive precipitation during the modeled period.

The outputs from the HCSS model, on the other hand, underestimated the evaporation amounts of water in all ponds when compared with estimates from the new model. This HCSS suggests that infiltration generally dominates water loss from these pond types which is not true for all cases. Here again, there is no discernable difference between the evaporation amounts and rates associated with the permanent, semi-permanent and the ephemeral ponds. Hence we cannot obtain any meaningful insights into the way these ponds function when the HCSS model is applied. The results suggest that the Craig and Gordon (1965) based models compiled in the H*ydrocalculator* software should not be applied to small ponds that lose water to infiltration, frequently dry up, and where isotopically distinct precipitation/inflows have a marked impact on the pond isotope composition.

Furthermore, the results of the individual flux estimates from the various classes of wetland ponds also suggest that the existing models predicted higher evaporation component in the smaller mostly the ephemeral and semi-permanent ponds, but almost the same evaporation for the larger permanent pond (pond 50, Table 4). These scenarios are expected in the models because the models have been designed to simulate relative component ratios for large lakes and rivers, where indeed precipitation additions and outflows balance inflows and have minimal effect. These results imply that while the precipitation additions, and pond size and shape play critical roles in the estimation of water balance components of small lakes and ponds that may not be the case for large lakes and rivers.

5.5. Model limitations

The model developed in this paper is useful for modelling stable isotope evolution with time in surface water and the estimation of evaporation and infiltration fluxes. This model is not capable of distinguishing how the infiltration flux is partitioned between transpiration (from the riparian zone and aquatic plants) and deeper groundwater recharge, which is essential for groundwater resources management in this region. In addition, the model does not represent surface water or groundwater inflows that may occur. Such additions could be included, but would require measurements of the amount of inflow and the isotopic composition of the inflowing water. This is generally not a problem in the Canadian prairies in the spring-summer period (after snowmelt has filled the ponds), where surface and groundwater inputs to the ponds are typically small in most years, but there will be times and places where the model cannot be applied.

The model does not take into account progressive changes in pond salinity, and local atmospheric conditions (e.g., relative humidity,

Table 4
Comparison of the evaporation amounts of the current model (PPM) with the steady-state (HCSS) and non-steady-state (HCNS) of modified Craig and Gordon (1965) and Gonfiantini (1986) computed with the Hydrocalculator software (Skrzypek et al., 2015).

	Pond	50				109				117	120
Model	Year	1994	1998	1999	2014	1994	1997	1998	2014	2014	2014
HCSS	***E (mm)***	116	24	97	7	190	18	44	38	29	97
HCNS	$\boldsymbol{E}$ (mm)	275	241	280	294	361	126	161	154	331	336
New	$\boldsymbol{E}$ (mm)	191	206	306	163	96	31	195	80	89	145

precipitation, temperature, solar radiation, and wind speed) which affect evaporation and evapotranspiration rates (Gonfiantini, 1986; Horita, 2009; Horita et al., 2008). Salinity effects can be worked into the model using the equations of Gonfiantini (1986) and the unified Craig-Gordon model (Gonfiantini et al., 2018).

One potential source of error in the model comes from the fact that the atmospheric water vapour composition was estimated based on the local evaporation line, which does not fully account for the local meteorological conditions that might be present (Gat and Levy, 1978; Steinman et al., 2010). The direct monitoring and measurement of relative humidity and atmospheric water vapour isotope composition could minimize this potential error.

6. Conclusions

Small wetland ponds are subject to significant seasonal fluctuations in water levels and isotope composition, due to their relatively short residence times. Our simple measurements of pond water isotope composition shows that such information can be used to estimate the hydrological fluxes into and out of the ponds and in particular to partition the water losses between evaporation and infiltration. We were able to show with the model how the infiltration rates varied between different types of pond, with higher infiltration rates in ephemeral ponds compared with permanent ponds. Future challenges for models like ours will be how to apportion infiltration from wetland ponds between plant transpiration vs groundwater recharge, and how to represent the effects of surface water and groundwater inflows into the ponds, where the amount and isotope composition of such waters are difficult to observe and quantify.

7. Declaration

The authors declare that they have no conflicting interest.

Author contributions

E.K.P.B. designed the study and field work, compiled each data set, did the geographic information system work, developed the equations, run the model and did the water balance and model comparison calculations, and wrote the original draft of paper. A.M.I, supervised and funded the research, wrote the python script and did sensitivity analysis reviewed the paper, and contributed to the text.

Acknowledgments

We thank the Canadian Wildlife Service for site access; the Internation Dean's scholarship program, University of Saskatchewan, Natural Sciences and Engineering Research Council, and Global Institute for Water Security for funding support. We thank Bob Clark, Randy Schmidt, and Heather Wilson for field assistance. We also thank Environment Canada for the archived data and Geoff Kohler and for making unpublished isotope data available. We thank Garth van der Kamp for useful comments along the way and three anonymous reviewers are thanked for their feedback that have helped improve the quality of this manuscript. We especially thank Jeff McDonnell for significant editing assistance and help throughout the study. This study is part of the first author's Ph.D. thesis at the University of Saskatchewan.

Appendix A. Supplementary data

Supplementary data to this article can be found online at https://doi.org/10.1016/j.jhydrol.2018.12.032.

References

Allen, R.G., Pereira, L.S., Raes, D., Smith, M., 1998. Crop evapotranspiration: guidelines for computing crop requirements. (No. 56). Irrig. Drainage. Rome, Italy. https://doi.org/10.1016/j.eja.2010.12.001.

Araguas-Araguas, L., Froehlich, K., Rozanski, K., 2000. Deuterium and oxygen-18 isotope composition of precipitation and atmospheric moisture. Hydrol. Process. 14, 1341–1355.

Bam, E.K.P., 2018. Understanding Hydrological Processes and Water Fluxes Linking Wetland Ponds and Groundwater in the Prairie Pothole Region (Ph.D. Thesis). University of Saskatchewan, Saskatoon (available at: https://harvest.usask.ca/handle/10388/8841).

Bam, E.K.P., Brannen, R., Budhathoki, S., Ireson, A.M., Spence, C., van der Kamp, G., 1Global, 2018. Meteorological, soil moisture, surface water, and groundwater data from the St Denis National Wildlife Area, Saskatchewan, Canada. Earth Syst. Sci. Data Discuss. https://doi.org/10.5194/essd-2018-125.

Begley, I.S., Scrimgeour, C.M., 1997. High-precision δ^2H and $\delta^{18}O$ measurement for water and volatile organic compounds by continuous-flow pyrolysis isotope ratio mass spectrometry. Anal. Chem. 69, 1530–1535. https://doi.org/10.1021/ac960935r.

Bennett, K.E., Gibson, J.J., McEachern, P.M., 2008. Water-yield estimates for critical loadings assessment: comparisons of gauging methods versus an isotopic approach. Can. J. Fish. Aquat. Sci. 65, 83–99. https://doi.org/10.1139/f07-155.

Benson, L.V., Paillet, F.L., 1989. The use of total lake-surface area as an indicator of climatic change: examples from the Lahontan basin. Quat. Res. 32, 262–275. https://doi.org/10.1016/0033-5894(89)90093-8.

Bortolotti, L.E., Clark, R.G., Wassenaar, L.I., 2013. Hydrogen isotope variability in prairie wetland systems: implications for studies of migratory connectivity. Ecol. Appl. 23, 110–121. https://doi.org/10.1890/12-0232.1.

Brannen, R., Spence, C., Ireson, A., 2015. Influence of shallow groundwater-surface water interactions on the hydrological connectivity and water budget of a wetland complex. Hydrol. Process. 29, 3862–3877. https://doi.org/10.1002/hyp.10563.

Clark, I., 2015. In: Groundwater Geochemistry and Isotopes, first ed. Taylor & Francis Group, LLC, Boca Raton. https://doi.org/10.1111/gwat.12377.

Clark, I., Fritz, P., 1997. Environmental Isotopes in Hydrogeology. Lewis Publishers, New York.

Coleman, M.L., Shepherd, T.J., Durham, J.J., Rouse, J.E., Moore, G.R., 1982. Reduction of water with zinc for hydrogen isotope analysis. Anal. Chem. 54, 993–995. https://doi.org/10.1021/ac00243a035.

Coles, A.E., McConkey, B.G., McDonnell, J.J., 2017. Climate change impacts on hillslope runoff on the northern Great Plains, 1962–2013. J. Hydrol. 550, 538–548. https://doi.org/10.1016/j.jhydrol.2017.05.023.

Conly, F.M., Su, M., van der Kamp, G., Millar, J.B., 2004. A practical approach to monitoring water levels in prairie wetlands. Wetlands 24, 219–226. https://doi.org/10.1672/0277-5212(2004) 024[0219:apatmw]2.0.co;2.

Coplen, T.B., 1988. Normalization of oxygen and hydrogen isotope data. Chem. Geol. 72, 293–297. https://doi.org/10.1016/0168-9622(88)90042-5.

Craig, H., Gordon, L.I., 1965. Deuterium and oxygen 18 variations in the ocean and the marine atmosphere. In: Tongiorgi, E. (Ed.), Stable Isot. Oceanogr. Stud. Paleotemp. SPOLETO, pp. 9–130.

Craig, H., Gordon, L.I., Horibe, Y., 1963. Isotopic exchange effects in the evaporation of water. J. Geophys. Res. 68, 5079–5087. https://doi.org/10.1029/JZ068i017p05079.

Cressey, R.L., Austin, J.E., Stafford, J.D., 2016. Three responses of wetland conditions to climatic extremes in the prairie pothole region. Wetlands 36, 357–370. https://doi.org/10.1007/s13157-016-0818-8.

Dansgard, W., 1964. Stable isotopes in precipitation. Tellus 4, 436–467. https://doi.org/10.1111/j.2153-3490.1964.tb00181.x.

Dincer, T., Hutton, L.G., Kupee, B.B.J., 1979. Study, using stable isotope, of flow distribution, surface -groundwater relations and evapotranspiration in the Okavango Swamp, Bostwana. In: Proceedings of an International Symposium on Isotope Hydrology Jointly Organized by the International Atomic Energy Agency and the United Nations Educational, Scientific and Cultural Organization and Held in Neuh Erberg, 19–23 June 1978. International Atomic Energy Agency, Vienna, pp. 3–29.

Dogramaci, S., Firmani, G., Hedley, P., Skrzypek, G., Grierson, P.F., 2015. Evaluating recharge to an ephemeral dryland stream using a hydraulic model and water, chloride and isotope mass balance. J. Hydrol. 521, 520–532. https://doi.org/10.1016/j.jhydrol.2014.12.017.

Eiler, J.M., Kitchen, N., 2001. Hydrogen-isotope analysis of nanomole (picoliter) quantities of H_2O. Geochem. Cosmochim. Acta 65, 4467–4479. https://doi.org/10.1021/jp312364c.

Epstein, S., Mayeda, T., 1953. Variation of ^{18}O content of waters from natural sources. Geochim. Cosmochim. Acta 4, 213–224. https://doi.org/10.1016/0016-7037(53)90051-9.

Fritz, P., Drimmie, R.J., Frape, S.K., O'Shea, K., 1987. The isotopic composition of precipitation and groundwater in Canada. Isot. Tech. Water Resour. Dev. 143, 539–549. https://doi.org/10.1016/0022-1694(93)90212-R.

Gammons, C.H., Poulson, S.R., Pellicori, D.A., Reed, P.J., Roesler, A.J., Petrescu, E.M., 2006. The hydrogen and oxygen isotopic composition of precipitation, evaporated mine water, and river water in Montana, USA. J. Hydrol. 328, 319–330. https://doi.org/10.1016/j.jhydrol.2005.12.005.

Gat, J.R., 2008. The isotopic composition of evaporating waters – review of the historical evolution leading up to the Craig-Gordon model. Isot. Environ. Health Stud. 44, 5–9. https://doi.org/10.1080/10256010801887067.

Gat, J.R., 1996. Oxygen and hydrogen isotopes in the hydrologic cycle. Annu. Rev. Earth Planet. Sci. 24, 225–262. https://doi.org/10.1146/annurev.earth.24.1.225.

Gat, J.R., 1995. Stable isotopes of fresh and saline lakes. Phys. Chem. Lakes. https://doi.

org/10.1016/0016-7037(96)83277-7.
Gat, J.R., Levy, Y., 1978. Isotope hydrology of inland sabkhas in the Bardawil area. Sinai. Limnol. Oceanogr. 23, 841–850. https://doi.org/10.4319/lo.1978.23.5.0841.
Geyh, M., D'Amore, F., Darling, G., Paces, T., Pang, Z., Šilar, J., 2000. Applications to low-temperature systems. In: Geyh, M. (Ed.), Environmental Isotopes in the Hydrological Cycle: Principles and Applications (Groundwater Saturated and Unsaturated Zone). International Atomic Energy Agency and United Nations Educational, Scientific and Cultural Organization, Hannover, pp. 1–291.
Gibson, J., 2002a. A new conceptual model for predicting isotopic enrichment of lakes in seasonal climates. Pages News 1–3.
Gibson, J.J., 2002b. Short-term evaporation and water budget comparisons in shallow Arctic lakes using non-steady isotope mass balance. J. Hydrol. 264, 242–261. https://doi.org/10.1016/S0022-1694(02)00091-4.
Gibson, J.J., Birks, S.J., Edwards, T.W.D., 2008a. Global prediction of δA and δ^2H-$\delta^{18}O$ evaporation slopes for lakes and soil water accounting for seasonality. Global Biogeochem. Cycl. 22, 1–12. https://doi.org/10.1029/2007GB002997.
Gibson, J.J., Birks, S.J., Yi, Y., 2016. Stable isotope mass balance of lakes: a contemporary perspective. Quat. Sci. Rev. 131, 316–328. https://doi.org/10.1016/j.quascirev.2015.04.013.
Gibson, J.J., Edward, T.W., Bursey, G.G., Prowse, T., 1993. Estimating evaporation using stable isotopes: quantitative results and sensitivity analysis for two catchments in northern Canada. Nord. Hidrol. 24, 79–94.
Gibson, J.J., Edwards, T.W.D., 2002. Regional water balance trends and evaporation-transpiration partitioning from a stable isotope survey of lakes in northern Canada. Global Biogeochem. Cycl. 16, 10–11. https://doi.org/10.1029/2001GB001839.
Gibson, J.J., Edwards, T.W.D., Birks, S.J., St Amour, N.A., Buhay, W.M., McEachern, P., Wolfe, B.B., Peters, D.L., 2005. Progress in isotope tracer hydrology in Canada. Hydrol. Process. 19, 303–327. https://doi.org/10.1002/hyp.5766.
Gibson, J.J., Edwards, T.W.D., Prowse, T.D., 1996. Development and validation of an isotopic method for estimating lake evaporation. Hydrol. Process. 10, 1369–1382. https://doi.org/10.1002/(SICI)1099-1085(199610)10:10<1369::AID-HYP467>3.0.CO;2-J.
Gibson, J.J., Reid, R., 2010. Stable isotope fingerprint of open-water evaporation losses and effective drainage area fluctuations in a subarctic shield watershed. J. Hydrol. 381, 142–150. https://doi.org/10.1016/j.jhydrol.2009.11.036.
Gibson, J.J., Reid, R., 2014. Water balance along a chain of tundra lakes: a 20-year isotopic perspective. J. Hydrol. 519, 2148–2164. https://doi.org/10.1016/j.jhydrol.2014.10.011.
Gibson, J.J., Sadek, M.A., Stone, D.J., Hughes, C.E., Hankin, S., Cendon, D.I., Hollins, S.E., 2008b. Evaporative isotope enrichment as a constraint on reach water balance along a dryland river. Isot. Environ. Health Stud. 44, 83–98. https://doi.org/10.1080/10256010801887489.
Gilath, C., Gonfiantini, R., 1983. Lake Dynamics, 1983rd ed., Guidebook on Nuclear Techniques in Hydrology. International Atomic Energy Agency, Vienna.
Goldhaber, M.B., Mills, C.T., Morrison, J.M., Stricker, C.A., Mushet, D.M., LaBaugh, J.W., 2014. Hydrogeochemistry of prairie pothole region wetlands: role of long-term critical zone processes. Chem. Geol. 387, 170–183. https://doi.org/10.1016/j.chemgeo.2014.08.023.
Goldhaber, M.B., Mills, C.T., Mushet, D.M., McCleskey, B.B., Rover, J., 2016. Controls on the geochemical evolution of prairie pothole region lakes and wetlands over decadal time scales. Wetlands 36, 255–272. https://doi.org/10.1007/s13157-016-0854-4.
Gonfiantini, R., 1986. Environmental isotopes in lake studies. In: Fritz, P., Fontes, J.-.C. (Eds.), Handbook of Environmental Isotope Geochemistry, The Terrestrial Environment. Elsevier, Amsterdam, pp. 113–168.
Gonfiantini, R., Wassenaar, L.I., Araguas-Araguas, L., Aggarwal, P., 2018. A unified Craig-Gordon isotope model of stable hydrogen and oxygen isotope fractionation during fresh or saltwater evaporation. Geochim. Cosmochim. Acta 30291–30296. https://doi.org/10.1016/j.gca.2018.05.020. https://do, S0016-7037(18)30291–6.
Granger, R.J., Gray, D.M., Dyck, G.E., 1984. Snowmelt infiltration to frozen Prairie soils. Can. J. Earth Sci. 21, 669–677. https://doi.org/10.1139/e84-073.
Hayashi, M., Van Der Kamp, G., 2000. Simple equations to represent the volume-area-depth relations of shallow wetlands in small topographic depressions. J. Hydrol. 237, 74–85. https://doi.org/10.1016/S0022-1694(00)00300-0.
Hayashi, M., van der Kamp, G., Rosenberry, D.O., 2016. Hydrology of Prairie Wetlands: understanding the integrated surface-water and groundwater processes. Wetlands 36, 237–254. https://doi.org/10.1007/s13157-016-0797-9.
Hayashi, M., van der Kamp, G., Rudolph, D.L.L., 1998. Water and solute transport between a prairie wetland and adjacent upland, 1. Water balance. J. Hydrol. 207, 42–55 doi: 1016/S0022-1694(98)00098-5.
Heagle, D., Hayashi, M., Kamp, G. Van Der, 2013. Surface–subsurface salinity distribution and exchange in a closed-basin prairie wetland. J. Hydrol. 478, 1–14. https://doi.org/10.1016/j.jhydrol.2012.05.054.
Heagle, D.J., 2008. Surface-subsurface Solute Cycling in Wetlands Receiving Groundwater Discharge. University of Calgary Ph.D.
Heagle, D.J., Hayashi, M., van der Kamp, G., 2007. Use of solute mass balance to quantify geochemical processes in a prairie recharge wetland. Wetlands 27, 806–818. https://doi.org/10.1672/0277-5212(2007) 27[806:UOSMBT]2.0.CO;2.
Horita, J., 2009. Isotopic evolution of saline lakes in the low-latitude and polar regions. Aquat. Geochem. 15, 43–69. https://doi.org/10.1007/s10498-008-9050-3.
Horita, J., Rozanski, K., Cohen, S., 2008. Isotope effects in the evaporation of water: a status report of the Craig-Gordon model. Isot. Environ. Health Stud. 44, 23–49. https://doi.org/10.1080/10256010801887174.
Horita, J., Wesolowski, D.J., 1994. Liquid-vapor fractionation of oxygen and hydrogen isotopes of water from the freezing to the critical temperature. Geochim. Cosmochim. Acta 58, 3425–3437. https://doi.org/10.1016/0016-7037(94)90096-5.
IAEA, 2009. Laser Spectroscopic Analysis of Liquid Water Samples for Stable Hydrogen and Oxygen Isotopes. Isot. Hydrol. Sect. Int. At. Energy Agency 49.
Jacob, H., Sonntag, C., 1991. An 8-year record of the seasonal variation of D and O-18 in atmospheric water vapour and precipitation at Heidelberg, Germany. Tellus. https://doi.org/10.1034/j.1600-0889.1991.t01-2-00003.x.
Jasechko, S., Sharp, Z.D., Gibson, J.J., Birks, S.J., Yi, Y., Fawcett, P.J., 2013. Terrestrial water fluxes dominated by transpiration. Nature 496, 347–350. https://doi.org/10.1038/nature11983.
Johnson, W.C., Werner, B., Guntenspergen, G.R., Voldseth, R.A., Millett, B., Naugle, D.E., Tulbure, M., Carroll, R.W.H., Tracy, J., Olawsky, C., 2010. Prairie wetland complexes as landscape functional units in a changing climate. Bioscience 60, 128–140. https://doi.org/10.1525/bio.2010.60.2.7.
Jolly, I.D., McEwan, K.L., Holland, K.L., 2008. A review of groundwater–surface water interactions in arid/semi-arid wetlands and the consequences of salinity for wetland ecology. Ecohydrology 1, 43–58. https://doi.org/10.1002/eco.
Jones, M.D., Imbers, J., 2010. Modeling Mediterranean lake isotope variability. Glob. Planet. Change 71, 193–200. https://doi.org/10.1016/j.gloplacha.2009.10.001.
Jones, M.D., Leng, M.J., Roberts, C.N., Türkeş, M., Moyeed, R., 2005. A coupled calibration and modelling approach to the understanding of dry-land lake oxygen isotope records. J. Paleolimnol. 34, 391–411. https://doi.org/10.1007/s10933-005-6743-0.
Karhu, J.A., 1997. Catalytic reduction of water to hydrogen for isotopic analysis using zinc containing traces of sodium. Anal. Chem. 69, 4728–4730. https://doi.org/10.1021/ac9704467.
Kelly, S.D., Heaton, K.D., Brereton, P., 2001. Deuterium/hydrogen isotope ratio measurement of water and organic samples by continuous-flow isotope ratio mass spectrometry using chromium as the reducing agent in an elemental analyser. Rapid Commun. Mass Spectrom. 15, 1283–1286. https://doi.org/10.1002/rcm.303.
Kumar, B., Nachiappan, R.P., 1999. On the sensitivity of Craig and Gordon model for the estimation of the isotopic composition of lake evaporates. Water Resour. Res. 35, 1689–1691. https://doi.org/10.1029/1999WR900011.
LaBaugh, J.W., Mushet, D.M., Rosenberry, D.O., Euliss, N.H., Goldhaber, M.B., Mills, C.T., Nelson, R.D., 2016. Changes in pond water levels and surface extent due to climate variability alter solute sources to closed-basin prairie-pothole wetland ponds, 1979 to 2012. Wetlands 36, 343–355. https://doi.org/10.1007/s13157-016-0808-x.
Labaugh, J.W., Rosenberry, D.O., Schuster, P.F., Reddy, M.M., Aiken, G.R., 1997. Hydrological and chemical estimates of the water balance of a closed basin lake in north central Minnesota. Water Resour. Res. 33, 2799–2812.
Labaugh, J.W., Winter, T.C., Rosenberry, D.O., 1998. Hydrologic functions of prairie wetlands. Great Plains Res. 8, 17–37.
Labaugh, J.W., Winter, T.C., Swanson, G.A., Rosenberry, D.O., Nelson, R.D., Euliss, N.H., 1996. Changes in atmospheric circulation patterns affect midcontinent wetlands sensitive to climate. Limnol. Oceanogr. 41, 864–870. https://doi.org/10.4319/lo.1996.41.5.0864.
Leibowitz, S.G., Mushet, D.M., Newton, W.E., 2016. Intermittent surface water connectivity: fill and spill vs Fill and Merge Dynamics. Wetlands 36, 323–342. https://doi.org/10.1007/s13157-016-0830-z.
Leibowitz, S.G., Vining, K.C., 2003. Temporal connectivity in a prairie pothole complex. Wetlands 23, 13–25. https://doi.org/10.1672/0277-5212(2003) 023.
Lis, G., Wassenaar, L.I., Hendry, M.J., 2008. High-precision laser spectroscopy D/H and $^{18}O/^{16}O$ measurements of microliter natural water samples. Anal. Chem. 80, 287–293. https://doi.org/10.1021/ac701716q.
Millar, J.B., 1971. Shoreline-area ratio as a factor in rate of water loss from small sloughs. J. Hydrol. 14, 259–284.
Mohammed, I.N., Tarboton, D.G., 2011. On the interaction between bathymetry and climate in the system dynamics and preferred levels of the Great Salt Lake. Water Resour. Res. 47, 1–15. https://doi.org/10.1029/2010WR009561.
Nachshon, U., Ireson, A., van der Kamp, G., Davies, S., Wheater, H.S., 2014. Impacts of climate variability on wetland salinization in the North American prairies. Hydrol. Earth Syst. Sci. 18, 1251–1263. https://doi.org/10.5194/hess-18-1251-2014.
Nachshon, U., Ireson, A., van der Kamp, G., Wheater, H.S., 2013. Sulfate salt dynamics in the glaciated plains of North America. J. Hydrol. 499, 188–199. https://doi.org/10.1016/j.jhydrol.2013.07.001.
Parsons, D.F., Hayashi, M., van der Kamp, G., 2004. Infiltration and solute transport under a seasonal wetland: bromide tracer experiments in Saskatoon, Canada. Hydrol. Process. 18, 2011–2027. https://doi.org/10.1002/hyp.1345.
Pennock, D., Bedard-Haughn, A., Kiss, J., van der Kamp, G., 2014. Application of hydropedology to predictive mapping of wetland soils in the Canadian Prairie Pothole Region. Geoderma 235–236, 199–211. https://doi.org/10.1016/j.geoderma.2014.07.008.
Pham, S.V., Leavitt, P.R., McGowan, S., Wissel, B., Wassenaar, L.I., 2009. Spatial and temporal variability of prairie lake hydrology as revealed using stable isotopes of hydrogen and oxygen. Limonol. Oceanogr. 54, 101–118. https://doi.org/10.4319/lo.2009.54.1.0101.
Rothfuss, Y., Biron, P., Braud, I., Canale, L., Durand, J.L., Gaudet, J.P., Richard, P., Vauclin, M., Bariac, T., 2010. Partitioning evapotranspiration fluxes into soil evaporation and plant transpiration using water stable isotopes under controlled conditions. Hydrol. Process. 24, 3177–3194. https://doi.org/10.1002/hyp.7743.
Rozanski, K., Araguás-Araguás, L., Gonfiantini, R., 1992. Relation between long-term trends of oxygen-18 isotope composition of precipitation and climate. Science 258, 981–985. https://doi.org/10.1126/science.258.5084.981.
Rozanski, K., Chmura, L., 2008. Isotope effects accompanying evaporation of water from leaky containers. Isot. Environ. Health Stud. 44, 51–59. https://doi.org/10.1080/10256010801887141.
Salama, R.B., Farrington, P., Bartle, G.A., Watson, G.D., 1993. Distribution of recharge and discharge areas in a first-order catchment as interpreted from water level patterns. J. Hydrol. 143, 259–277. https://doi.org/10.1016/0022-1694(93)90195-F.
Skrzypek, G., Mydłowski, A., Dogramaci, S., Hedley, P., Gibson, J.J., Grierson, P.F., 2015.

Estimation of evaporative loss based on the stable isotope composition of water using Hydrocalculator. J. Hydrol. 523, 781–789. https://doi.org/10.1016/j.jhydrol.2015.02.010.
Sloan, C., 1972. In: Ground-water Hydrology of Prairie Potholes in North Dakota, pp. 1–29.
Socki, R.A., 1999. On-line technique for measuring stable oxygen and hydrogen isotopes from microliter quantities of water. Anal. Chem. 71, 2250–2253. https://doi.org/10.1021/ac981140i.
Spence, C., 2010. A paradigm shift in hydrology: storage thresholds across scales influence catchment-runoff generation. Geogr. Compass 47 (7), 819–833.
Spence, C., Woo, M.-K., 2003. Hydrology of subarctic Canadian shield: soil-filled valleys. J. Hydrol. 279, 151–156.
Steinman, B.A., Rosenmeier, M.F., Abbott, M.B., Bain, D.J., 2010. The isotopic and hydrologic response of small, closed-basin lakes to climate forcing from predictive models: application to paleoclimate studies in the upper Columbia River basin. Limnol. Oceanogr. 55, 2231–2245. https://doi.org/10.4319/lo.2010.55.6.2231.
Stewart, R.E., Kantrud, H.A., 1971. Classification of Natural Ponds and Lakes in the Glaciated Prairie Region. Resource Publication 92.
van der Kamp, G., Hayashi, M.M., 2009. Groundwater-wetland ecosystem interaction in the semiarid glaciated plains of North America. Hydrogeol. J. 17, 203–214. https://doi.org/10.1007/s10040-008-0367-1.
van der Kamp, G., Keir, D., Evans, M.S., 2008. Long-term water level changes in closed-basin lakes of the Canadian Prairies. Can. Water Resour. 33, 23–38. https://doi.org/10.4296/cwrj3301023.
Waiser, M.J., 2006. Relationship between hydrological characteristics and dissolved organic carbon concentration and mass in northern prairie wetlands using a conservative tracer approach. J. Geophys. Res. Biogeosci. 111, 1–15. https://doi.org/10.1029/2005JG000088.
Wassenaar, L.I., Athanasopoulos, P., Hendry, M.J., 2011. Isotope hydrology of precipitation, surface and ground waters in the Okanagan Valley, British Columbia, Canada. J. Hydrol. 411, 37–48. https://doi.org/10.1016/j.jhydrol.2011.09.032.
Winter, T.C., 2000. The vulnerability of wetlands to climate change: a hydrologic landscape perspective. J. Am. Water Resour. Assoc. 36, 305–311. https://doi.org/10.1111/j.1752-1688.2000.tb04269.x.
Winter, T.C., Rosenberry, D.O., 1998. Hydrology of Prairie pothole wetlands during drought and deluge: a 17 year study of the cottonwood lake wetland complex in North dakota in the perspective of longer term measured and proxy hydrological records. Clim. Change 189–209.
Wittrock, V., Beaulieu, C., 2015. Climate Reference Station Saskatoon Annual Summary 2014, Saskatoon Saskatchewan.
Woo, M.K., Rowsell, R.D., 1993. Hydrology of a prairie slough. J. Hydrol. 146, 175–207. https://doi.org/10.1016/0022-1694(93)90275-E.
Yepez, E.A., Williams, D.G., Scott, R.L., Lin, G., 2003. Partitioning overstory and understory evapotranspiration in a semiarid savanna woodland from the isotopic composition of water vapor. Agric. Meteorol. 119, 53–68. https://doi.org/10.1016/S0168-1923(03)00116-3.